Alumoxanes as Cocatalysts in the Palladium-Catalyzed Copolymerization of Carbon Monoxide and Ethylene: Genesis of a Structure−Activity Relationship

Yoshihiro Koide,[1a] Simon G. Bott,[1b] and Andrew R. Barron*,[1a]

Departments of Chemistry, Rice University, Houston, Texas 77005, and University of North Texas, Denton, Texas 76203

Received October 27, 1995[⊗]

The palladium-catalyzed copolymerization of carbon monoxide and ethylene to give polyketone polymers, $[CH_2CH_2C(O)]_n$, has been accomplished by the use of either (dppp)-$Pd(OAc)_2$ or (dppp)$Pd[C(O)^tBu]Cl$ in the presence of a *tert*-butyl alumoxane, $[(^tBu)Al(\mu_3\text{-}O)]_n$ (n = 6, 7, 9) or $[(^tBu)_7Al_5(\mu_3\text{-}O)_3(\mu\text{-}OH)_2]$ cocatalyst. The effects on the catalytic activity of the alumoxane and palladium concentrations, the alumoxane structure, and the identity of the phosphine ligands were determined. The function of the alumoxane is shown to depend on the choice of palladium catalyst precursor. With (dppp)$Pd[C(O)^tBu]Cl$ the alumoxane abstracts chloride to give a catalytically active cationic palladium complex directly. In contrast, the alumoxane initially alkylates the palladium in (dppp)$Pd(OAc)_2$ and subsequently abstracts the remaining acetate anion, yielding the active cationic palladium complex. The catalytic activity is highly dependent on the structure of the alumoxane. A comparative study indicates the cocatalytic activity to be $[(^tBu)Al(\mu_3\text{-}O)]_7 > [(^tBu)Al(\mu_3\text{-}O)]_6 > [(^tBu)Al(\mu_3\text{-}O)]_9 \gg [(^tBu)_7Al_5(\mu_3\text{-}O)_3(\mu\text{-}OH)_2]$. This observed cocatalytic activity correlates with the predicted latent Lewis acidity of the alumoxanes. A discussion of the palladium−alumoxane complex is presented with respect to the model compound $[(^tBu)_6Al_6(\mu_3\text{-}O)_4(\mu\text{-}OH)_2(\mu\text{-}O_2CCCl_3)_2]$, prepared by the reaction of $[(^tBu)Al(\mu_3\text{-}O)]_6$ with HO_2CCCl_3. The steric effects of the catalyst active site, as determined by the alkyl bridge length (n) in $R_2P(CH_2)_nPR_2$ and the alkyl substituents R, were probed for the catalyst precursor compounds $[R_2P(CH_2)_n\text{-}PR_2]Pd[C(O)^tBu]Cl$ (R = Ph, n = 2 (dppe), 3 (dppp), 4 (dppb); R = Me (dmpe), C_6H_{11} (dcpe), n = 2). The concept of "pocket angle" has been developed to account for the observed steric effects. The detection of vinyl end groups on low-molecular-weight oligomers is indicative of catalyst turnover via a β-hydride-elimination chain termination. A proposed catalyst mechanism and a pathway to catalyst activation are presented. The molecular structures of (dppp)$Pd[C(O)^tBu]Cl$, (dppe)$Pd[C(O)^tBu]Cl$, (dmpe)$Pd[C(O)^tBu]Cl$, (dcpe)$Pd[C(O)^tBu]Cl$, and $[(^tBu)_6Al_6(\mu_3\text{-}O)_4(\mu\text{-}OH)_2(\mu\text{-}O_2CCCl_3)_2]$ have been determined by X-ray crystallography.

Introduction

The palladium-catalyzed copolymerization of olefins and carbon monoxide to form polyketone polymers is well established. The cationic palladium phosphine catalysts commonly employed may either be preformed, e.g., $[Pd(PPh_3)_n(MeCN)_{4-n}][BF_4]$,[2,3] or formed in situ from the reaction of $[R_2P(CH_2)_3PR_2]Pd(OAc)_2$ with non-coordinating acids (e.g., HBF_4).[4] Despite the diversity of polyketone catalyst systems reported, all are based upon a cationic transition-metal center, $[L_nMX]^+$, and a non-coordinating anion.[5−9]

We have recently reported that polyketone polymers may be synthesized using a palladium catalyst, (dppp)-$Pd(OAc)_2$ or (dppp)$Pd[C(O)^tBu]Cl$, with an isolable *tert*-butyl alumoxane cocatalyst, $[(^tBu)Al(\mu_3\text{-}O)]_6$ (eq 1).[10] The polymers are perfectly alternating ethylene/CO, have high molecular weights (16 700 < M_n < 58 400), and show no spectroscopic evidence for furanization or cross-linking.[11]

$$H_2C{=}CH_2 + CO \xrightarrow[\text{alumoxane}]{\text{Pd-catalyst}} \left(CH_2{-}CH_2{-}\overset{\overset{O}{\|}}{C}\right)_n \qquad (1)$$

The function of the alumoxane cocatalyst was intended to mimic the noncoordinating anion in the more traditional palladium catalyst systems. However, we have recently shown that in the case of zirconocene-catalyzed polymerization of ethylene the alumoxane is not an innocent noncoordinating anion but has a

* To whom all correspondence should be addressed.
⊗ Abstract published in *Advance ACS Abstracts,* April 15, 1996.

(1) (a) Rice University. (b) University of North Texas.
(2) Sen, A.; Lai, T. *J. Am. Chem. Soc.* **1982**, *104*, 3520.
(3) Lai, T.; Sen, A. *Organometallics* **1984**, *3*, 866.
(4) See for example: (a) Drent, E.; Wife, R. L. U.S. Patent 4,970,-294, 1990. (b) Van Leeuwen, P. W. N.; Roobeek, C. F.; Wong, P. K. Eur. Pat. Appl. EP 393,790, 1990. (c) Drent, E. Eur. Pat. Appl. EP 390,292, 1990.
(5) See: (a) Brookhart, M.; Grant, B.; Volpe, A. F., Jr. *Organometallics* **1992**, *11*, 3920. (b) Brookhart, M.; Rix, F. C.; DeSimone, J. M.; Barborak, J. C. *J. Am. Chem. Soc.* **1992**, *114*, 5894.
(6) Drent, E.; Van Broekhoven, J. A. M.; Doyle, M. J. *J. Organomet. Chem.* **1991**, *417*, 235.
(7) Chepaikin, E. G.; Bezruchenko, A. P.; Belov, G. P. *Izv. Akad. Nauk SSSR, Ser. Khim.* **1990**, *9*, 2181.
(8) Sen, A.; Jiang, Z. *Macromolecules* **1993**, *26*, 911.
(9) Klaubunde, U.; Tulip, T. H.; Roe, D. C.; Ittel, S. D. *J. Organomet. Chem.* **1987**, *334*, 141.
(10) Koide, Y.; Barron, A. R. *Macromolecules* **1996**, *29*, 1110.
(11) Koide, Y.; Barron, A. R. *Main Group Met. Chem.* **1995**, *18*, 405.

S0276-7333(95)00849-1 CCC: $12.00

contributory role in the polymerization due to its complexation to the zirconium center.[12] Furthermore, we proposed that the cocatalytic activity of each alumoxane, $[(^t\text{Bu})\text{Al}(\mu_3\text{-O})]_n$ ($n = 6-9$), can be related to its structure as measured by the latent Lewis acidity.[13] On the basis of our results with the Cp_2ZrMe_2/alumoxane-catalyzed polymerization of ethylene, it seems reasonable to expect that the alumoxane function in the palladium-catalyzed copolymerization of ethylene and CO also be nonbenign. In this regard we have investigated the effects on the catalytic activity of the alumoxane and palladium concentrations, the alumoxane structure, and the identity of the phosphine ligands. The results of this study are reported herein.

Results and Discussion

In our preliminary experiments we adapted the literature catalyst system, by reaction of $(dppp)Pd(OAc)_2$ (**I**) with a mixture of *tert*-butyl alumoxanes, $[(^t\text{Bu})\text{Al}(\mu_3\text{-O})]_n$, in place of the acid cocatalyst. $(dppp)Pd(OAc)_2$ was replaced with the palladium pivaloyl compound $(dppp)Pd[C(O)^t\text{Bu}]Cl$ (**II**) to simplify the catalyst initiation reaction. Previous studies have shown that $(Ph_3P)_2Pd[C(O)Me]Cl$ is a precursor to an active catalyst upon addition of $AgBF_4$.[3] In subsequent experiments the mixture of alumoxanes was substituted by a single isomer, $[(^t\text{Bu})\text{Al}(\mu_3\text{-O})]_n$, ($n = 6$ (**III**),[14] 7 (**IV**),[15] 9 (**V**)[14]) and $[Al_5(^t\text{Bu})_7(\mu_3\text{-O})_3(\mu\text{-OH})_2]$ (**VI**).[15]

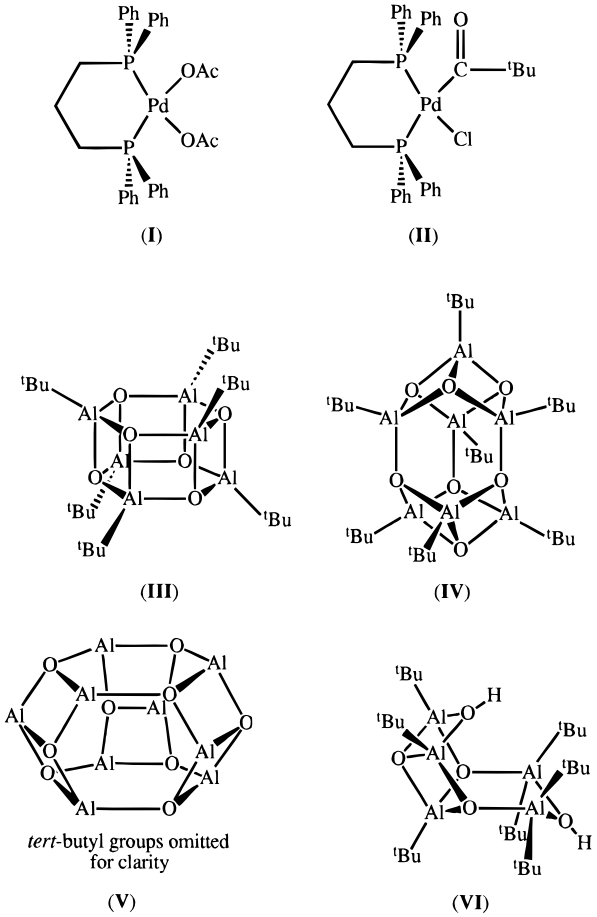

As a general procedure, a CH_2Cl_2 solution of alumoxane was added to a solution of the palladium catalyst, previously purged with CO, in a Teflon-lined autoclave (see Experimental Section). The reaction mixture was then pressurized to 300 psi[16] with an equimolar mixture of CO and ethylene and heated to 60 °C. The pressure of the vessel was monitored during the course of the reaction. The reaction was quenched by release of the CO/ethylene pressure upon completion of the polymerization. The polymer was isolated by filtration and washing.

All of the polyketone polymers isolated are white, independent of catalyst or reaction pressure.[10] Spectroscopically the polyketone polymers prepared using alumoxane cocatalysts are identical with those previously reported;[17] however, all the polymers prepared using alumoxane cocatalysts are stable high-density modifications of the α-phase.[18] Full spectroscopic and structural characterization data have been reported elsewhere.[10]

Catalytic Dependence on Alumoxane. We have previously shown there to be a strong structural dependence for individual alumoxanes on the catalytic activity in the ring-opening polymerization of β-lactones[19] and the zirconocene−alumoxane polymerization of ethylene.[12] Furthermore, we have attempted to correlate this structural dependence with the latent Lewis acidity of the Al−O cages, as well as with the steric strain in the anionic product.[12]

In order to determine the effect of the alumoxane structure on the catalytic activity of the palladium-catalyzed copolymerization of CO and ethylene, we have investigated the rate of polymerization using four different alumoxanes. The alumoxanes investigated are $[(^t\text{Bu})\text{Al}(\mu_3\text{-O})]_6$ (**III**), $[(^t\text{Bu})\text{Al}(\mu_3\text{-O})]_7$ (**IV**), $[(^t\text{Bu})\text{Al}(\mu_3\text{-O})]_9$ (**V**), and $[(^t\text{Bu})_7Al_5(\mu_3\text{-O})_3(\mu\text{-OH})_2]$ (**VI**).

As can be seen from Figure 1, the relative rates of activity are $[(^t\text{Bu})\text{Al}(\mu_3\text{-O})]_7 > [(^t\text{Bu})\text{Al}(\mu_3\text{-O})]_6 > [(^t\text{Bu})\text{Al}(\mu_3\text{-O})]_9 \gg [(^t\text{Bu})_7Al_5(\mu_3\text{-O})_3(\mu\text{-OH})_2]$. The observed cocatalytic activity correlates well with the predicted latent Lewis acidity of the alumoxanes.[12] Furthermore, the relative activity of the alumoxanes remains constant throughout catalysis. In each case a large excess of alumoxane was employed ([alumoxane] = 10[Pd]; see below). The observation of a correlation between alumoxane structure and sustained catalytic activity is important and suggests that the alumoxane is not a spectator counterion but is actively involved in the activity of the catalyst site. Further evidence for the active role of the alumoxane is the concentration dependence of the alumoxane on the rate of polymerization.

(12) Harlan, C. J.; Bott, S. G.; Barron, A. R. *J. Am. Chem. Soc.* **1995**, *117*, 6465.

(13) We have defined latent Lewis acidity to be the ability of electron-precise cage compounds to act as Lewis acids upon cage opening. The extent of latent Lewis acidity is dependent on the ring strain within the cage.

(14) Mason, M. R.; Smith, J. M.; Bott, S. G.; Barron, A. R. *J. Am. Chem. Soc.* **1993**, *115*, 4971.

(15) Harlan, C. J.; Mason, M. R.; Barron, A. R. *Organometallics* **1994**, *13*, 2957.

(16) 100 psi = 5170 Torr = 6.89 bar.

(17) Lommerts, B. J.; Klop, E. A.; Aerts, J. *J. Polym. Sci., Polym. Phys.* **1993**, *31*, 1319.

(18) Polyketone, prepared from carbon monoxide and ethylene, is known to crystallize in two forms: an α- and a β-phase. There is, however, some disagreement as to the relationship of the phases. Several workers have proposed that the β-phase is a high-temperature form of the α-phase. Alternatively, it has been proposed that the change in crystal structure is due to defects in the chains introduced upon heating; see: Chatani, Y.; Takizawa, T.; Murahashi, S.; Sakata, Y.; Nishimura, Y. *J. Polym. Sci.* **1961**, *55*, 811.

(19) Wu, B.; Lenz, R. W.; Harlan, C. J.; Barron, A. R. *Can. J. Microbiol.* **1995**, *41*, 274.

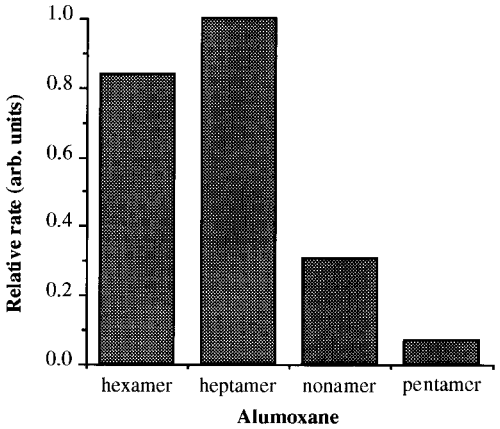

Figure 1. Relative catalytic activity as a function of the alumoxanes $[(^t\text{Bu})\text{Al}(\mu_3\text{-O})]_6$ (hexamer), $[(^t\text{Bu})\text{Al}(\mu_3\text{-O})]_7$ (heptamer), $[(^t\text{Bu})\text{Al}(\mu_3\text{-O})]_9$ (nonamer), and $[(^t\text{Bu})_7\text{Al}_5(\mu_3\text{-O})_3(\mu\text{-OH})_2]$ (pentamer). In all reactions $(\text{dppp})\text{Pd}(\text{OAc})_2$ was used as the palladium source.

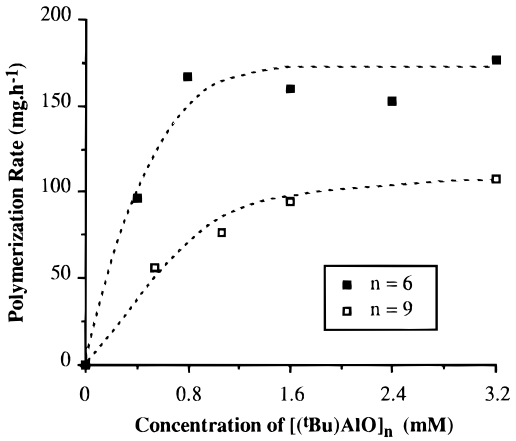

Figure 2. Polyketone yield as a function of $[(^t\text{Bu})\text{Al}(\mu_3\text{-O})]_6$ concentration (mM), relative to a constant concentration of $(\text{dppp})\text{Pd}(\text{OAc})_2$ (0.16 mM). All reactions were performed over 2 h at 60 °C and 300 psi (CO, ethylene).

The dependence of the rate of polyketone synthesis on the alumoxane concentration was determined for both $[(^t\text{Bu})\text{Al}(\mu_3\text{-O})]_6$ and $[(^t\text{Bu})\text{Al}(\mu_3\text{-O})]_9$: $T = 60$ °C, $P_i = 300$ psi, $[(\text{dppp})\text{Pd}(\text{OAc})_2] = 0.16$ mM. As can be seen from Figure 2, the polymerization rate increases as the alumoxane concentration is increased relative to that of palladium. The catalytic activity appears to reaches a maximum with a large excess of alumoxane, suggesting that all the palladium centers are activated.[20] However, two important points should be noted. First, even under conditions of large excess, $[(^t\text{Bu})\text{Al}(\mu_3\text{-O})]_6$ is more reactive than $[(^t\text{Bu})\text{Al}(\mu_3\text{-O})]_9$. Second, the relative alumoxane concentration to reach maximum activity is lower for $[(^t\text{Bu})\text{Al}(\mu_3\text{-O})]_6$ than for $[(^t\text{Bu})\text{Al}(\mu_3\text{-O})]_9$. Possible explanations for these observations are discussed below.

While $[(^t\text{Bu})\text{Al}(\mu_3\text{-O})]_7$ is slightly more active than $[(^t\text{Bu})\text{Al}(\mu_3\text{-O})]_6$, the ease of synthesis of the latter as compared to the former determined that all subsequent experiments were performed with pure $[(^t\text{Bu})\text{Al}(\mu_3\text{-O})]_6$.

(20) Under our conditions, there is sometimes a decrease in the polymer yield at higher alumoxane concentrations. This observation is contrary to expectations and is possibly indicative of the instability of the palladium−alumoxane complex, in the absence of ethylene/CO.

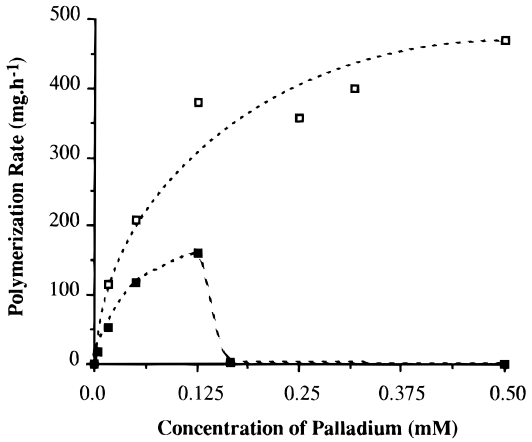

Figure 3. Polyketone yield as a function of palladium concentration (mM), relative to a constant concentration of $[(^t\text{Bu})\text{Al}(\mu_3\text{-O})]_6$ (0.25 mM): (■) $(\text{dppp})\text{Pd}(\text{OAc})_2$; (□) $(\text{dppp})\text{Pd}[\text{C(O)}^t\text{Bu}]\text{Cl}$. The reactions were performed over 2 h at 60 °C and 300 psi (CO, ethylene).

Catalytic Dependence on Palladium. The polymer yield increases with increased $(\text{dppp})\text{Pd}(\text{OAc})_2$ concentration in the presence of an excess of the alumoxane $[(^t\text{Bu})\text{Al}(\mu_3\text{-O})]_6$ (see Figure 3). This is consistent with each palladium producing a single active site. Clearly, catalysis is not due to a minor contaminant or metallic palladium formed by thermal or reductive decomposition. A maximum catalytic activity is observed for a $(\text{dppp})\text{Pd}(\text{OAc})_2$/alumoxane molar ratio of 0.5, which indicates that two molecules of $[(^t\text{Bu})\text{Al}(\mu_3\text{-O})]_6$ per $(\text{dppp})\text{Pd}(\text{OAc})_2$ are required for the formation of the catalytically active species. Such an observation is consistent with a two-step reaction between $(\text{dppp})\text{Pd}(\text{OAc})_2$ and two molecules of $[(^t\text{Bu})\text{Al}(\mu_3\text{-O})]_6$; the first equivalent of alumoxane reacts with the palladium via metathesis of one acetate group (eq 2),

$$(\text{dppp})\text{Pd}(\text{OAc})_2 + [(^t\text{Bu})\text{Al}(\mu_3\text{-O})]_6 \rightarrow (\text{dppp})\text{Pd}(^t\text{Bu})(\text{OAc}) + [(^t\text{Bu})_5\text{Al}_6(\text{O})_6(\text{OAc})] \quad (2)$$

$$(\text{dppp})\text{Pd}(^t\text{Bu})(\text{OAc}) + [(^t\text{Bu})\text{Al}(\mu_3\text{-O})]_6 \rightarrow [(\text{dppp})\text{Pd}(^t\text{Bu})]^+ + [(^t\text{Bu})_6\text{Al}_6(\text{O})_6(\text{OAc})]^- \quad (3)$$

and the second alumoxane is required to abstract the remaining acetate group to form a cationic palladium complex similar to that previously proposed as the active catalyst (eq 3). If an excess of $(\text{dppp})\text{Pd}(\text{OAc})_2$ is used, then the catalytic activity is close to zero. This observation suggests that $(\text{dppp})\text{Pd}(\text{OAc})_2$ reacts with the active catalyst (see below).

We presume that no reaction occurs between the carboxyl-substituted alumoxane formed from the metathesis of the first acetate, $[(^t\text{Bu})_5\text{Al}_6(\text{O})_6(\text{OAc})]$, and the palladium alkyl acetate $(\text{dppp})\text{Pd}(^t\text{Bu})(\text{OAc})$. Attempts to prepare $(\text{dppp})\text{Pd}(^t\text{Bu})(\text{OAc})$, from the reaction of $(\text{dppp})\text{Pd}(\text{OAc})_2$ and $^t\text{BuMgCl}$, to test this hypothesis were unsuccessful (see Experimental Section).

If, of the two alumoxanes required for catalysis, the first alkylates the palladium and the second abstracts the acetate to yield a cationic species, then if $(\text{dppp})\text{Pd}[\text{C(O)}^t\text{Bu}]\text{Cl}$ (**II**) is used in place of $(\text{dppp})\text{Pd}(\text{OAc})_2$ only one alumoxane should be required to produce an active catalyst. This is indeed observed, as shown in Figure 3. As with $(\text{dppp})\text{Pd}(\text{OAc})_2$ the polymer yield

increases with increased (dppp)Pd[C(O)^{t}Bu]Cl concentration until the Pd/alumoxane ratio is *ca.* 1, at which point catalysis reaches a maximum. The fact that the catalysis reaches a maximum at one alumoxane per palladium suggests that each alumoxane is only able to react with 1 equiv of (dppp)Pd[C(O)^{t}Bu]Cl. However, at higher palladium concentrations catalysis remains constant. This is unlike the Cp_2ZrMe_2/[(^{t}Bu)Al(μ_3-O)]$_6$-catalyzed polymerization of ethylene, where we have evidence that each [(^{t}Bu)Al(μ_3-O)]$_6$ can react with two Cp_2ZrMe_2 molecules.[12]

It is interesting to note that the absolute yield of polyketone appears to be greater using (dppp)Pd[C(O)^{t}Bu]Cl than (dppp)Pd(OAc)$_2$, even under optimum conditions for each palladium catalyst precursor. This is presumably related to either the magnitude of the equilibrium constant between the neutral and "cationic" palladium complexes (eq 4; X = Cl, OAc) or the coordinating ability of the resulting alumoxane complex [(^{t}Bu)$_6$Al$_6$(O)$_6$(X)]$^-$ (X = Cl versus OAc). The reversible nature of this type of reaction has been observed previously.[12]

$$(\text{dppp})\text{Pd(P)X} + [(^t\text{Bu})\text{Al}(\mu_3\text{-O})]_6 \rightleftharpoons [(\text{dppp})\text{Pd(P)}]^+ + [(^t\text{Bu})_6\text{Al}_6(\text{O})_6(\text{X})]^- \quad (4)$$

$$\text{P} = \text{polymer}$$

Catalytic Dependence on the Phosphine Ligand. Several groups have reported a significant effect on catalytic activity of the chelate ring size (as determined by the alkyl bridge length *n*) for a number of catalytic systems containing bidentate phosphines, $R_2P(CH_2)_nPR_2$: e.g., the rhodium-catalyzed hydrogenation of styrene.[21] In the case of palladium-catalyzed polyketone synthesis, Drent and co-workers[6] observed that the maximum activity and highest molecular weights were obtained by the use of a propyl-bridged diphosphine; i.e., $n = 3$. These workers suggested that the control exerted by the phosphine was due to the ability of the diphosphine to stabilize both square-planar and trigonal-bipyramidal geometries, the maximum activity being observed for phosphines in which the bite angle (P−Pd−P) allows complexation in both geometries. Subsequently, Chien and co-workers observed the same trend in catalytic activity but proposed an alternative rationale based upon the ability of the various phosphines to undergo chelate opening.[22]

To determine how the steric and electronic properties of the phosphine ligand effect the catalytic activity in the alumoxane cocatalyzed system, we systematically varied the chelate ring size (*n*), and the alkyl substituents (R), for the catalyst precursor compounds [$R_2P(CH_2)_nPR_2$]Pd[C(O)^{t}Bu]Cl. A comparison of the relative catalytic activity of (dppp)Pd[C(O)^{t}Bu]Cl (**II**) with (dppe)Pd[C(O)^{t}Bu]Cl (**VII**; dppe = 1,2-bis(diphenylphosphino)ethane) and (dppb)Pd[C(O)^{t}Bu]Cl (**VIII**; dppe = 1,2-bis(diphenylphosphino)butane) will determine the effect of phosphine chelate ring size. Similarly, a comparison of the catalytic activity of (dppe)Pd[C(O)^{t}Bu]Cl with that of (dmpe)Pd[C(O)^{t}Bu]Cl (dmpe = 1,2-bis(dimethylphosphino)ethane) and (dcpe)Pd[C(O)^{t}Bu]Cl (dppe = 1,2-bis(dicyclohexylphosphino)ethane) allows for the effects of alkyl substitution to be probed.

Table 1. Relative Catalytic Activity and Estimated Interior Cone Angle as a Function of the Phosphine Ligand in [$R_2P(CH_2)_nPR_2$]Pd[C(O)^{t}Bu]Cl

phosphine[a]	n[b]	initial rate dP/dt (psi·min^{-1})	total polymer yield[c] (g)	$\theta_{\|\|}$[d] (deg)	$\theta_{\perp}$[e] (deg)
dppe	2	0.19	0.216	132	129
dppp	3	0.75	1.42	108	146
dppb	4	0.12	0.025	93	102
dmpe	2		none	141	174
dcpe	2	0.83	1.25	106	115

[a] Abbreviations: dppe = 1,2-bis(diphenylphosphino)ethane, dppp = 1,3-bis(diphenylphosphino)propane, dppb = 1,4-bis(diphenylphosphino)butane, dmpe = 1,2-bis(dimethylphosphino)ethane, dcpe = 1,2-bis(dicyclohexylphosphino)ethane. [b] $R_2P(CH_2)_nPR_2$. [c] After 10 h. [d] Parallel to the PdP_2 plane. [e] Perpendicular to the PdP_2 plane.

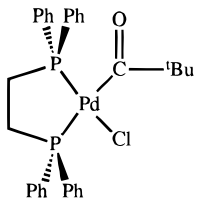

(**VII**)

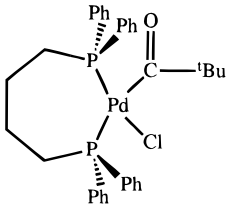

(**VIII**)

The relative catalytic activity of each compound was determined with [(^{t}Bu)AlO]$_6$ as the cocatalyst (see Table 1). In addition, the molecular structures of (dppp)Pd[C(O)^{t}Bu]Cl, (dppe)Pd[C(O)^{t}Bu]Cl, (dmpe)Pd[C(O)^{t}Bu]Cl, and (dcpe)Pd[C(O)^{t}Bu]Cl were determined by X-ray crystallography (see below).

The relative rate of catalysis and total polymer yield as a function of the phosphine in [$Ph_2P(CH_2)_nPPh_2$]Pd[C(O)^{t}Bu]Cl follow the order previously observed for the acid cocatalyzed catalysts; i.e., $n = 3 > 2 > 4$.[6] However, (dmpe)Pd[C(O)^{t}Bu]Cl shows almost no activity, even for oligomer formation, and (dcpe)Pd[C(O)^{t}Bu]Cl exhibits an activity comparable to that of (dppp)Pd[C(O)^{t}Bu]Cl. These latter observations are contrary to both of the proposed structure−activity relationships.[6,22] Clearly, if chelate ring size is the most important factor in controlling catalyst activity, then (dmpe)Pd[C(O)^{t}Bu]Cl, (dppe)Pd[C(O)^{t}Bu]Cl, and (dcpe)Pd[C(O)^{t}Bu]Cl should be comparable catalysts, which they are not. Similarly, if chelate opening is the controlling effect, then the more basic the phosphine, the lower its activity should be; i.e., dppe > dmpe > dcpe. However, this trend is not observed. Thus, an alternative explanation must be sought.

It is clear that for the ethylene-bridged phosphines (dmpe, dppe, and dcpe) catalytic activity increases with the increased steric bulk of the phosphine's alkyl substituents, as mirrored by the increasing alkyl cone angles: Me in dmpe (90°), Ph in dppe (105°), and C_6H_{11} in dcpe (117°).[23] Furthermore, increasing the length of the phosphine backbone not only increases the bite angle of the phosphine but also forces the phenyl substituents toward the palladium, as indicated by a decrease in the average Pd−P−Ph angle measured from

(21) Poulin, J.-C.; Dang, T.-P.; Kagan, H. B. *J. Organomet. Chem.* **1975**, *84*, 87.
(22) Xu, F. Y.; Zhao, A. X.; Chien, J. C. W. *Makromol. Chem.* **1993**, *194*, 2579.
(23) Tolman, C. A. *Chem. Rev.* **1977**, *77*, 313.

the solid-state structures (see below): 117° in (dppe)Pd[C(O)^{t}Bu], 114° in (dppp)Pd[C(O)^{t}Bu]Cl, and 113° in (dppb)PdX_2 (estimated[24]). Thus, increasing the length of the phosphine's backbone results in increased steric crowding at the palladium. Given the foregoing, it would seem reasonable that some form of steric control is in operation.

While the steric bulk of monodentate phosphines is readily estimated by Tolman's cone angle,[23] there has been no simple method to estimate the steric effects of bidentate phosphines. Using the space-filling models derived from crystallographic data, it is difficult to compare the steric hindrance of the "pocket" in the dppe, dppp, and dppb complexes. It is desirable, therefore, to derive a semiquantitative measure of the size of the active site at palladium.

If we assume that the P−C bonds in $[Ph_2P(CH_2)_n PPh_2]PdX_2$ compounds are free to rotate, then if solid-state structures of $[Ph_2P(CH_2)_nPPh_2]$Pd[C(O)^{t}Bu]Cl are used as models (see below), a measure may be made of the pocket angle at palladium:[25] both parallel ($\theta_{||}$, **IX**) and perpendicular ($\theta_\perp$, **X**) to the PdP_2 plane. The

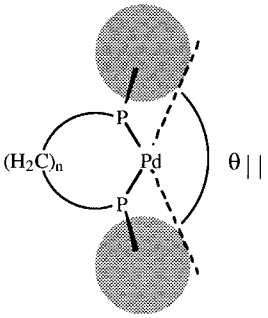

(**IX**)

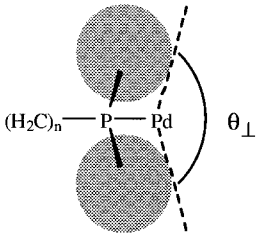

(**X**)

parallel pocket angle ($\theta_{||}$) is defined as the angle subtended between two planes perpendicular to the PdP_2 plane, and bisecting at the metal, that can exclude the van der Waals surface of all the ligands over all rotational orientations about the P−C bonds. Similarly, the perpendicular pocket angle ($\theta_\perp$) is defined as the angle subtended between two planes parallel with the P_2 vector, and bisecting at the metal, that can exclude the van der Waals surface of all the ligands over all rotational orientations about the P−C bonds. Calculated values for $\theta_{||}$ and $\theta_\perp$ are given in Table 1.[26]

From Table 1 it can be clearly seen that there is an optimum size for the active site. Furthermore, catalysis is primarily dependent on the size of the interior cone angle in the plane of the ligands around palladium, i.e., $\theta_{||}$. This is not surprising, since the most sterically crowded species during the catalytic cycle is the ethylene complex $[\{Ph_2P(CH_2)_nPPh_2\}Pd(H_2C{=}CH_2)C(O)R]^+$, formed as an intermediate prior to olefin insertion. In order for olefin insertion/acyl migration to occur, the ethylene must be coplanar with the migrating acyl group, shown in **XI**.[27] Thus, it is in the ligand plane

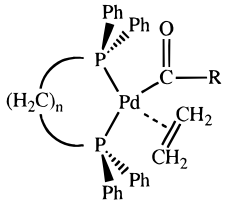

(**XI**)

that steric hindrance becomes a controlling factor in ethylene coordination/insertion.

It is reasonable to propose that if the internal cone angle of the $[Ph_2P(CH_2)_nPPh_2]$Pd moiety is sufficiently small (i.e., $n = 4$), then ethylene is precluded from complexation: the equilibrium shown in eq 5 is shifted predominantly to the left. However, it is not imme-

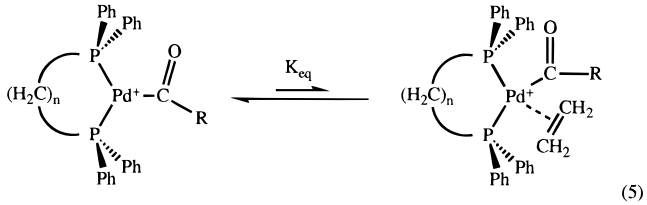

(5)

diately obvious why little or no catalytic activity is observed for large phosphine pocket angles at palladium, such as in the case of (dppe)Pd[C(O)^{t}Bu]Cl and (dmpe)Pd[C(O)^{t}Bu]Cl. The following explanations are consistent with observation and literature precedent. (1) The lack of steric hindrance about palladium provides a facile pathway for the decomposition of the active catalyst. This is consistent with the observation of palladium metal during reactions using (dmpe)Pd[C(O)^{t}Bu]Cl; however, little palladium metal is observed during reactions using (dppe)Pd[C(O)^{t}Bu]Cl. (2) The formation of stable metallocycles of the type shown in Scheme 1 have been reported for the insertion of norbornadiene.[28] Such chelate formation will oppose the insertion of the next monomer unit (carbon monoxide) by blocking the required coordination site on palladium and thus inhibiting polymerization (Scheme 1). The magnitude of this effect will depend on the coordination strength of the carbonyl group β to the palladium center. The relative stability of such a chelate ligand will be dependent on the effectiveness of the carbonyl oxygen−palladium electrostatic interaction, which will be determined by the chelate ring size (in the present case independent of the phosphine ligand) and the steric hindrance of the phosphine ligand. For complexes in which the phosphine has a small pocket angle (i.e., dppp, dcpe) the phosphine's substituents may inhibit, or even preclude, chelation as a consequence of the steric

(24) We have been unable to obtain crystals of (dppb)Pd[C(O)^{t}Bu]Cl suitable for X-ray crystallography. Thus, the Pd−P−Ph angles and pocket angles were determined from related structures; see: (a) Haggerty, B. S.; Housecroft, C. E.; Rheingold, A. L.; Shaykh, B. A. M. *J. Chem. Soc., Dalton Trans.* **1991**, 2175. (b) Werner, H.; Ebner, M.; Bertleff, W.; Schubert, U. *Organometallics* **1983**, *2*, 891. (c) Ganter, C.; Orpen, A. G.; Bergamini, P.; Costa, E. *Acta Crystallogr., Sect. C* **1994**, *C50*, 507.

(25) We have defined the "pocket angle" to be the interior cone angle of a chelating phosphine.

(26) The pocket angles given in Table 1 are calculated from X-ray crystal structures of the palladium complexes; however, similar values are obtained by assuming a generic M−P bond distance of 2.28 Å, as is done for cone angle measurements; *cf.* ref 23.

(27) Hoffmann et al. have shown that the thermodynamically stable conformation of a palladium olefin complex is with the olefin bound perpendicular to the P_2PdL_2 plane; see: Albright, T. A.; Hoffmann, R.; Thibeault, J. C.; Thorn, D. L. *J. Am. Chem. Soc.* **1979**, *101*, 3801. However, the ethylene must be coplanar with the acyl group for migration to occur: Hoffmann, R. *J. Am. Chem. Soc.* **1978**, *100*, 2079.

(28) (a) van Asselt, R.; Gielens, E. C. G.; Rülke, R. E.; Vrieze. K.; Elsevier, C. J. *J. Am. Chem. Soc.* **1994**, *116*, 977. (b) Brumbaugh, J. S.; Whittle, R. R.; Parvez, M. A.; Sen, A. *Organometallics* **1990**, *9*, 1735.

Scheme 1. Suggested Chelate Formation for Palladium Complexes with a Sufficiently Large Phosphine Pocket Angle

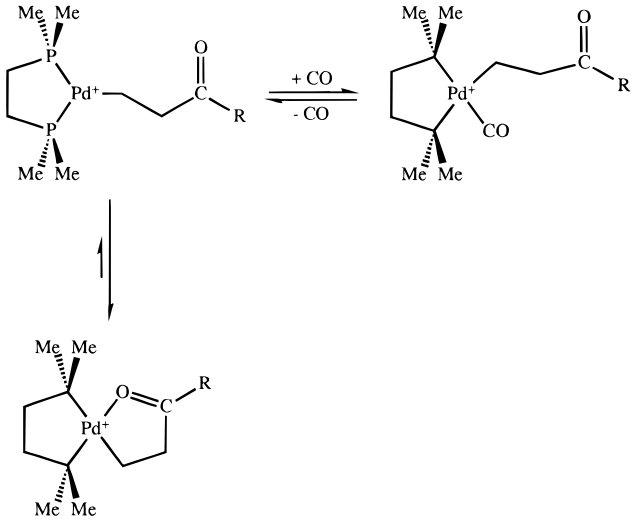

repulsion between the alkyl substituents on phosphorus and the carbonyl. In contrast, complexes containing phosphines with a large pocket angle (i.e., dmpe) will have significantly less steric hindrance, and chelation may become so strong that the insertion of the next monomer is inhibited completely; therefore, chain propagation cannot occur. This rationalization would also provide a plausible explanation for the formation of oligomer with the dppe ligand.

While our results agree with these explanations, other possibilities may exist. What is clear, however, is the importance of the size (steric hindrance) and possibly shape of the active catalytic site in these palladium complexes.

Molecular Structures of $[R_2P(CH_2)_nPR_2]Pd[C(O)^tBu]Cl$. The molecular structures of (dppp)Pd[C(O)^{t}Bu]Cl, (dppe)Pd[C(O)^{t}Bu]Cl, (dmpe)Pd[C(O)^{t}Bu]Cl, and (dcpe)Pd[C(O)^{t}Bu]Cl are shown in Figures 4−7, respectively; selected bond lengths and angles are given in Table 2.

The palladium centers are, as expected, essentially square planar; i.e., $\sum(X-Pd-Y) = 359.1(2)-360.0(1)°$. As can be seen from Table 2, the chelate phosphine's bite angle, P(1)−Pd(1)−P(2), is only dependent on the magnitude of the Pd−P−C_n−P cycle. A similar trend has been reported for $[R_2P(CH_2)_nPR_2]PdCl_2$ compounds.[29] In contrast, the Cl(1)−Pd(1)−C(1) angle is independent of the phosphine bite angle and appears to depend on the conformation of the phosphine's alkyl substituents. Thus, while the Cl(1)−Pd(1)−C(1) angles in (dppp)Pd[C(O)^{t}Bu]Cl and (dppe)Pd[C(O)^{t}Bu]Cl are similar, those in (dmpe)Pd[C(O)^{t}Bu]Cl and (dcpe)Pd[C(O)^{t}Bu]Cl are significantly larger. It is clear from Figure 7 that in the solid state two of the cyclohexyl groups in (dcpe)Pd[C(O)^{t}Bu]Cl are positioned to minimize steric interaction with the pivaloyl and chloride ligands,[30] resulting in a Cl(1)−Pd(1)−C(1) angle similar to that in (dmpe)Pd[C(O)^{t}Bu]Cl. This is in contrast to the observed solution steric hindrance of the dcpe ligand in catalysis (see above).

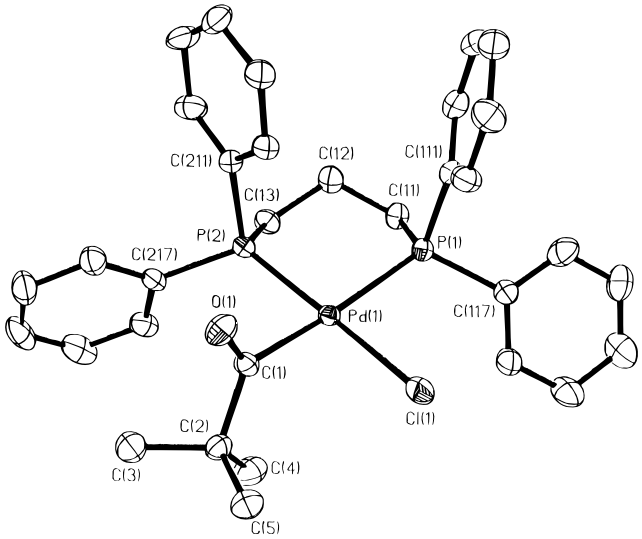

Figure 4. Molecular structure of (dppp)Pd[C(O)^{t}Bu]Cl. Thermal ellipsoids are shown at the 30% level, and hydrogen atoms are omitted for clarity.

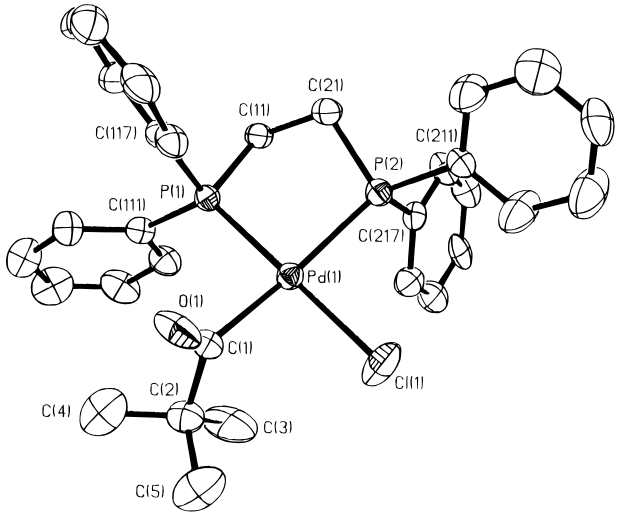

Figure 5. Molecular structure of (dppe)Pd[C(O)^{t}Bu]Cl. Thermal ellipsoids are shown at the 30% level, and hydrogen atoms are omitted for clarity.

The Pd−P bond distances fall into two distinct groups: those *trans* to the chloride (2.247(2)−2.254(1) Å) and those *trans* to the pivaloyl group (2.366(1)−2.409(2) Å), consistent with the greater *trans* influence exerted by the latter. It has previously been reported[31] that the M−P bond distance in metallacyclic compounds is related to the number of atoms in the metallacycle. A similar trend is observed for (dppp)Pd[C(O)^{t}Bu]Cl versus (dppe)Pd[C(O)^{t}Bu]Cl, (dmpe)Pd[C(O)^{t}Bu]Cl, and (dcpe)Pd[C(O)^{t}Bu]Cl (see Table 2). The Pd(1)−C(1) distances (2.038(5)−2.071(4) Å) are slightly shorter than previously reported values for Pd−alkyl (2.08−2.09 Å),[32] concordant with the σ-donor ability of an acyl being stronger than that of an alkyl substituent. The Pd(1)−Cl(1) distances are within the range expected; however, an interesting correlation is observed: the Pd−Cl bond distance is inversely proportional to the *trans*-P−Pd−

(29) Steffen, W. L.; Palenik, G. J. *Inorg. Chem.* **1976**, *15*, 2432.
(30) A similar confirmation was previously observed for (dcpe)$PdCl_2$; see: Ganguly, S.; Mague, J. T.; Roundhill, D. M. *Acta Crystallogr., Sect. C* **1994**, *C50*, 217.
(31) Ros, R.; Lenarda, M.; Pahor, N. B.; Calligaris, M.; Delise, P.; Randaccio, L.; Graziani, M. *J. Chem. Soc., Dalton Trans.* **1976**, 1937.
(32) See for example: (a) Wisner, J. M.; Bartczark, T. J.; Ibers, J. A. *Organometallics* **1986**, *5*, 2044. (b) de Graaf, W.; Boersma, J.; Smeets, W. J. J.; Spek, A. L.; van Koten, G. *Organometallics* **1989**, *8*, 2907.

Table 2. Selected Bond Lengths (Å) and Angles (deg) for $[R_2P(CH_2)_nPR_2]Pd[C(O)^tBu]Cl$

	phosphine			
	dppp	dppe	dmpe	dcpe
Pd(1)−Cl(1)	2.386(2)	2.362(3)	2.382(2)	2.380(1)
Pd(1)−P(1)	2.409(2)	2.247(2)	2.340(2)	2.254(1)
Pd(1)−P(2)	2.254(1)	2.377(2)	2.229(2)	2.366(1)
Pd(1)−C(1)	2.038(5)	2.042(8)	2.041(7)	2.071(4)
P(1)−C(11)	1.815(6)	1.838(8)	1.81(1)	1.845(5)
P(1)−C(111)	1.819(5)	1.812(9)	1.81(1)	1.831(4)
P(1)−C(117)	1.834(6)	1.824(9)	1.784(8) [C(112)]	1.843(5)
P(2)−C(21)	1.828(6) [C(13)]	1.815(8)	1.82(1)	1.836(5)
P(2)−C(211)	1.828(5)	1.816(9)	1.81(1)	1.834(4)
P(2)−C(217)	1.818(6)	1.825(9)	1.786(9) [C(212)]	1.848(4)
O(1)−C(1)	1.194(6)	1.18(1)	1.204(9)	1.193(5)
C(1)−C(2)	1.552(8)	1.53(1)	1.55(1)	1.563(6)
Cl(1)−Pd(1)−P(1)	92.51(5)	179.69(9)	91.42(7)	173.99(5)
Cl(1)−Pd(1)−P(2)	173.08(5)	94.74(9)	177.07(7)	89.06(5)
Cl(1)−Pd(1)−C(1)	85.7(2)	86.7(2)	91.7(2)	90.8(1)
P(1)−Pd(1)−P(2)	91.58(5)	85.57(7)	85.66(7)	86.63(4)
P(1)−Pd(1)−C(1)	170.8(1)	93.0(2)	174.2(2)	92.9(1)
P(2)−Pd(1)−C(1)	89.4(2)	173.9(3)	91.2(2)	171.7(1)
Pd(1)−P(1)−C(11)	116.7(2)	106.7(2)	106.3(3)	109.0(2)
Pd(1)−P(1)−C(111)	107.9(2)	120.3(3)	118.1(3)	111.8(1)
Pd(1)−P(1)−C(117)	121.1(2)	114.4(2)	117.8(3) [C(112)]	121.7(2)
Pd(1)−P(2)−C(21)	115.4(2) [C(13)]	104.6(3)	108.0(3)	106.5(1)
Pd(1)−P(2)−C(211)	109.4(2)	120.1(3)	120.7(4)	119.1(1)
Pd(1)−P(2)−C(217)	120.9(2)	115.6(3)	115.9(3) [C(212)]	115.1(1)
Pd(1)−C(1)−O(1)	118.4(4)	118.4(7)	118.4(6)	118.9(3)
Pd(1)−C(1)−C(2)	121.5(3)	121.5(6)	122.4(5)	122.5(3)
O(1)−C(1)−C(2)	119.9(5)	119.9(8)	119.1(6)	118.1(4)

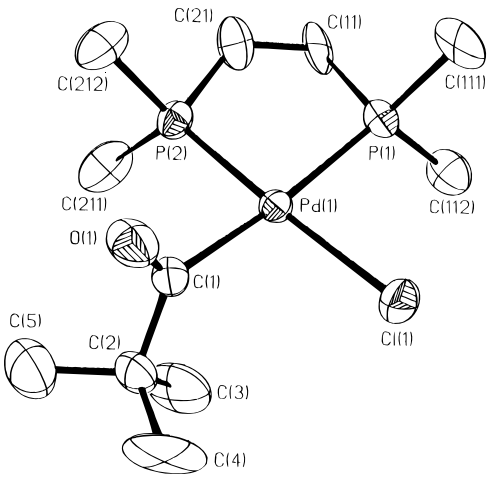

Figure 6. Molecular structure of (dmpe)Pd[C(O)^{t}Bu]Cl. Thermal ellipsoids are shown at the 30% level, and hydrogen atoms are omitted for clarity.

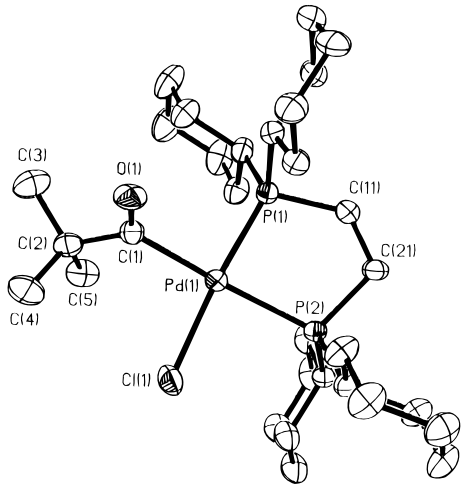

Figure 7. Molecular structure of (dcpe)Pd[C(O)^{t}Bu]Cl. Thermal ellipsoids are shown at the 30% level, and hydrogen atoms are omitted for clarity.

Cl angle. Such a correlation is the obverse of that expected from *trans*-influence arguments: i.e., the closer a ligand is to being *trans*, the longer the metal−ligand bond distance.[33] In the present case the correlation is consistent with an orbital overlap argument: the closer to linear the P−Pd−Cl vector, the greater the σ-bonding overlap between the ligand donor orbital and the palladium $d_{x^2-y^2}$.

The six-membered PdP_2C_3 ring in (dppp)Pd[C(O)^{t}Bu]-Cl is in a chair conformation, resulting in the axial−equatorial arrangement of the phenyl groups.[34] The five-membered Pd−P−C−C−P rings in (dppe)Pd[C(O)-^{t}Bu]Cl, (dmpe)Pd[C(O)^{t}Bu]Cl, and (dcpe)Pd[C(O)^{t}Bu]Cl are all puckered due to the preference of the PCH_2CH_2P moiety for a staggered conformation.[35] In all the structures the pivaloyl group is oriented out of the palladium coordination plane to reduce steric congestion.

Polyketone Polymer End-Group Analysis. While the formation of the α-phase of polyketone clearly indicates that the polymerization reaction involves the alternating insertion of carbon monoxide and ethylene, the high molecular weights obtained ($16\,700 < M_n < 58\,400$) precluded spectroscopic identification of the end

(33) See for example: (a) Lyons, D.; Wilkinson, G.; Thornton-Pett, M.; Hursthouse, M. B. *J. Chem. Soc., Dalton Trans.* **1984**, 695. (b) Barron, A. R.; Wilkinson, G.; Motevalli, M.; Hursthouse, M. B. *J. Chem. Soc., Dalton Trans.* **1987**, 837.

(34) Hermann, W. A.; Brossmer, C.; Priermeier, T.; Öfele, K. *J. Organomet. Chem.* **1994**, *481*, 97.

(35) See for example: (a) Salt, J. E.; Girolami, G. S.; Wilkinson, G.; Motevalli, M.; Thornton-Pett, M.; Hursthouse, M. B. *J. Chem. Soc., Dalton Trans.* **1985**, 685. (b) Girolami, G. S.; Wilkinson, G.; Galas, A. M. R.; Thornton-Pett, M.; Hursthouse, M. B. *J. Chem. Soc., Dalton Trans.* **1985**, 1339. (c) Salt, J. E.; Wilkinson, G.; Motevalli, M.; Hursthouse, M. B. *J. Chem. Soc., Dalton Trans.* **1986**, 1141. (d) Barron, A. R.; Salt, J. E.; Girolami, G. S.; Wilkinson, G.; Motevalli, M.; Hursthouse, M. B. *J. Chem. Soc., Dalton Trans.* **1987**, 2947.

groups. Such information would allow an understanding of the initiation and chain-termination steps. Furthermore, the presence of a chain-termination step not associated with the hydrolytic workup of the polymer should indicate that catalyst turnover is occurring.

While the concentration dependence on the alumoxane and palladium in the (dppp)Pd(OAc)$_2$ system indicates that the alumoxane performs two functions to initiate the catalyst, the use of the pivaloyl substituent in the (dppp)Pd[C(O)^{t}Bu]Cl catalyst precursor should preform the growth chain. It may be presumed that upon chloride abstraction the initial reaction would involve ethylene insertion (eq 6). If this is indeed true,

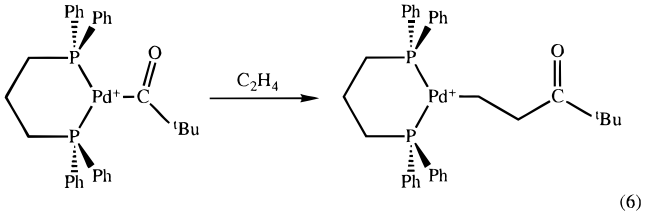

then the resulting polymers will be terminated by a C(O)^{t}Bu group. We were unsuccessful in the observation of such pivaloyl end groups by ^{1}H NMR.[10] However, oligomers were isolated by limiting the reaction times to 15 min and removing insoluble polymers prior to analysis (see Experimental Section).

The soluble oligomeric species formed using (dppp)Pd[C(O)^{t}Bu]Cl and [(^{t}Bu)Al(μ_3-O)]$_6$ were characterized by ^{1}H and ^{13}C NMR spectroscopy. The ^{13}C NMR spectrum, by comparison with that of *bona fide* spectra of ^{t}BuC(O)R groups, is consistent with the presence of a C(O)^{t}Bu-terminated polymer (see Experimental Section). Furthermore, the GC−mass spectrum of the volatile oligomers shows the predominant species to be the polyketone **XII**. Phenyl end groups are observed for oligomeric species formed using (dppp)Pd[C(O)Ph]Cl (see Experimental Section).

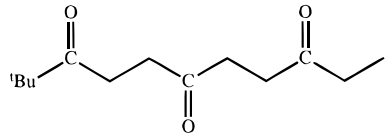

(**XII**)

No oligomers with *tert*-butyl groups were observed when (dppp)Pd(OAc)$_2$ was used as the palladium precursor, as either ^{t}BuC(O)− or ^{t}BuCH$_2$CH$_2$C(O)− termini. The ^{13}C NMR and mass spectra of the products formed during short reaction times show the presence of two types of oligomers: saturated oligo-ketones EtC(O)[(C$_2$H$_4$)C(O)]$_n$Et (**XIII**), and oligomers with ethyl terminal groups (**XIV**). The formation of ethyl-terminated oligomers indicates that the polymers are not formed via a palladium pivaloyl complex. Instead, initiation of polymerization must occur in the following sequence: metathetical alkylation of palladium by the alumoxane, abstraction of acetate, β-hydride elimination of the *tert*-butyl group to yield a hydride, and ethylene insertion. The active catalyst is therefore [(dppp)PdH]$^+$. In this manner the alumoxane cocatalyzed polymerization is analogous to that observed for the (dppp)Pd(OAc)$_2$/HX system.[4] The oligomers observed for reactions using (dppp)Pd[C(O)Et]Cl as the catalyst precursor are identical with those observed using (dppp)Pd(OAc)$_2$ (see Experimental Section).

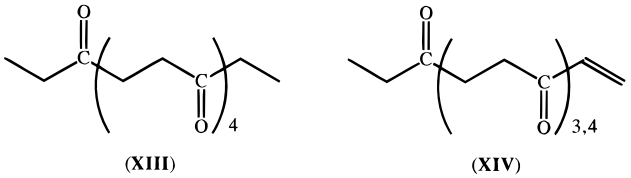

(**XIII**) (**XIV**)

In all of the oligomers, termination is observed to be *via* an alkyl or olefinic group. The alkyl is formed upon alcoholysis of the living polymer species upon ethanol workup (see Experimental Section) (eq 7), while the olefinic group is formed as a result of β-hydride elimination (eq 8). The observation of oligomeric β-hydride elimination products suggests that catalysis turnover occurs even after only a few CO/ethylene insertion steps. The result of a single catalyst turnover is, thus, the formation of the cationic palladium hydride [(dppp)PdH]$^+$, similar to that proposed for the (dppp)Pd(OAc)$_2$/HX system.

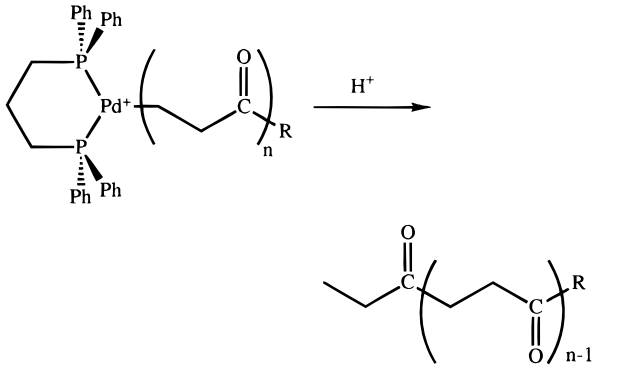

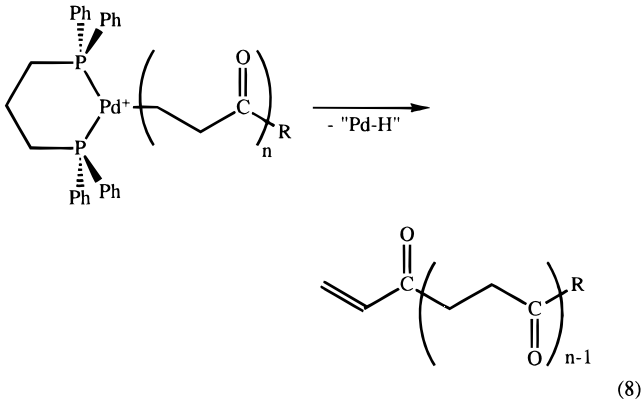

It is important to note that there is no evidence for aldehyde termination upon hydrolysis, consistent with the reversible CO insertion:[5b,28] releasing the CO pressure after polymerization leads to decarbonylation of Pd−acyl to result in Pd−alkyl, which by either solvolysis or β-hydride elimination gives the ethyl ketone or vinyl ketone end group, respectively.

Chain Initiation, Propagation, and Termination Mechanisms. On the basis of the foregoing experimental data the palladium/alumoxane-catalyzed copolymerization of ethylene and carbon monoxide is proposed to occur in the manner summarized in Scheme 2.

Catalyst initiation via the formation of a palladium hydride has been previously observed for polyketone

Scheme 2. Proposed Catalyst Formation and Catalytic Cycle for Palladium−Alumoxane Copolymerization of Olefins and Carbon Monoxide

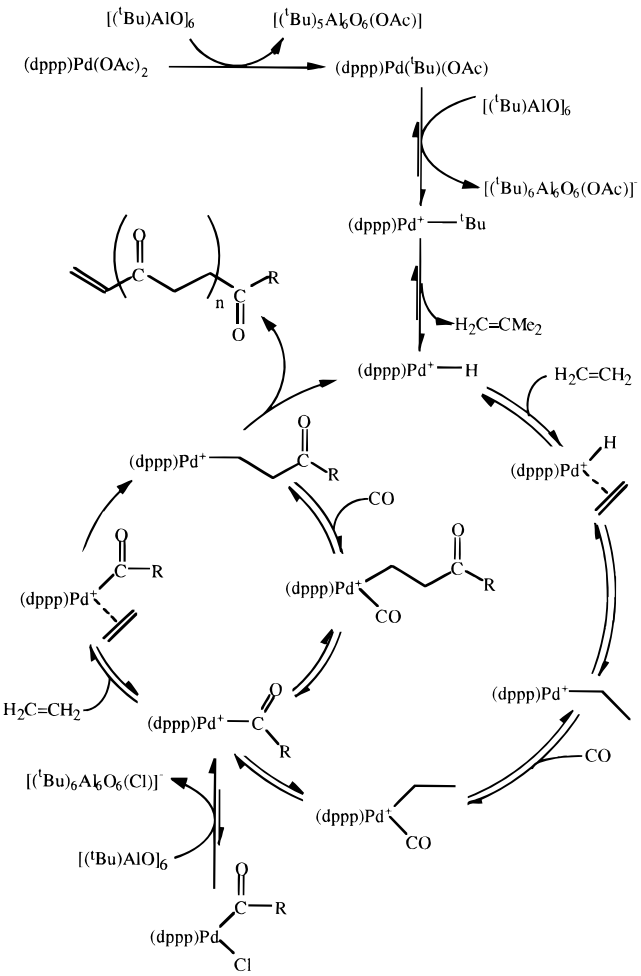

synthesis using cationic palladium catalysts in both protic[3] and aprotic solvents.[36] In the alumoxane cocatalyzed system, use of $(dppp)Pd(OAc)_2$ as the catalyst precursor also involves hydride formation. As is shown in Scheme 2, reaction of $(dppp)Pd(OAc)_2$ with 2 molar equiv of $[(^tBu)Al(\mu_3\text{-}O)]_n$ results in the following: (1) metathetical exchange of acetate for *tert*-butyl (eq 2), (2) abstraction of the remaining acetate anion (eq 3), and (3) β-hydride elimination. The alumoxane products formed in the first and second reaction steps are, in the case of the hexamer, $[(^tBu)_5Al_6(O)_6(OAc)]$ and $[(^tBu)_6Al_6(O)_6(OAc)]^-$, respectively. The requirement of two alumoxanes per palladium precludes $[(^tBu)_5Al_6O_6(OAc)]$ from abstracting the second acetate; i.e., the reaction shown in eq 9 does not occur. The lack of evidence for

$$[(^tBu)_5Al_6(O)_6(OAc)] + (dppp)Pd(^tBu)(OAc) \not\rightarrow [(^tBu)_5Al_6(O)_6(OAc)_2]^- + [(dppp)Pd(^tBu)]^+ \quad (9)$$

any *tert*-butyl end groups for polymers or oligomers formed using $(dppp)Pd(OAc)_2$ suggests that either CO insertion into the $Pd-C(CH_3)_3$ group is not favored or the β-hydride elimination reaction is faster than carbonyl insertion. If $(dppp)Pd[C(O)^tBu]Cl$ is used as the catalyst precursor, then only a single equivalent of alumoxane is required to activate the complex, via chloride abstraction (cf. eq 4). A similar palladium acyl catalyst has been reported.[3] Once catalysis is initiated, both palladium precursors result in similar products, the only difference being that $(dppp)Pd[C(O)^tBu]Cl$ yields 1 molar equiv of a pivaloyl-terminated polymer per palladium.

There have been several detailed studies of the chain propagation mechanism of metal-catalyzed copolymerization of olefins with CO.[37] The accepted mechanism, especially in aprotic solvents,[38] involves the alternate insertion of CO and the olefin into a preformed Pd−alkyl bond.[3,5b,39] By analogy with these previous studies we propose that a similar mechanism is applicable for the alumoxane cocatalyzed system (see Scheme 2). Given the similarity of chain propagation and catalyst initiation, it would be expected that chain termination occurs in a manner similar to that for previous aprotic catalyst systems (i.e., via β-hydride elimination and solvolysis upon reaction workup); this is indeed observed.

Catalyst Speciation. On the basis of the similarity in chain initiation, propagation, and termination steps with those of the traditional palladium cationic polymerization catalysts, we may expect that the alumoxane cocatalyst represents an alternative route to the $[(dppp)Pd(R)]^+$ complexes. The function of the alumoxane would therefore be simply as a source of a noncoordinating anion (e.g., $[(^tBu)_6Al_6(O)_6(X)]^-$; X = Cl, OAc) and, thus, be a direct replacement for the traditional counterions (e.g., $[BF_4]^-$, $[O_3STol]^-$, $[O_3SCF_3]^-$, etc.) employed in polyketone synthesis.[2−4] Given our previous results which demonstrate that the cage structure of the alumoxane opens to accept an anionic ligand, a structure such as **XV** may be reasonably proposed for the alumoxane counterion formed from the hexamer.

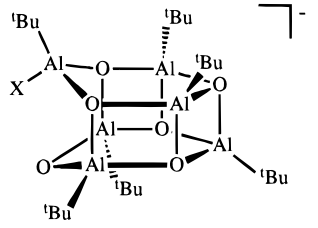

X = Cl, OAc (**XV**)

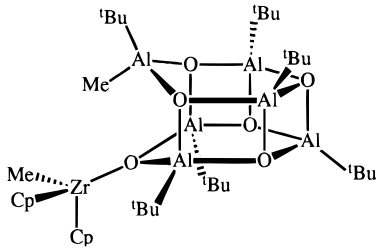

(**XVI**)

(36) (a) Jiang, Z.; Dahlen, G. M.; Houseknecht, K.; Sen, A. *Polym. Prepr., Am. Chem. Soc., Div. Polym. Chem.* **1992**, *33*, 1233. (b) Jiang, Z.; Dahlen, G. M.; Houseknecht, K.; Sen, A. *Macromolecules* **1992**, *25*, 2999.

(37) For a recent review, see: Sen, A. *Acc. Chem. Res.* **1993**, *26*, 303.

(38) A mechanism involving cationic Pd−carbene species has been proposed for the copolymerization of propylene with CO; see: Batistini, A.; Consiglio, G. *Organometallics* **1992**, *11*, 1766.

(39) With regard to the alkyl to acyl reaction step (Scheme 1), recent studies have demonstrated that alkyl migration rather than carbonyl insertion is the preferred mechanism for cationic palladium complexes: van Leeuwen, P. W. N. M.; Roobeek, C. F.; van der Heijden, H. *J. Am. Chem. Soc.* **1994**, *116*, 12117.

Any difference in activity between the alumoxanes, $[(^t\mathrm{Bu})\mathrm{Al}(\mu_3\text{-}\mathrm{O})]_n$, would have to be based upon any variation in the coordinating ability of each of the resulting alumoxane anions, $[(^t\mathrm{Bu})_n\mathrm{Al}_n(\mathrm{O})_n\mathrm{X}]^-$.

It has been previously assumed that the function of alumoxanes as cocatalysts in the Ziegler−Natta type polymerization of olefins also involves the formation of a noncoordinating anion.[40−43] However, we have recently demonstrated that the alumoxanes do not form simple noncoordinating anions but act as ligands to the metal center to form a discrete complex, e.g., **XVI**.[13] Given our previous results, it is possible that a similar situation could apply for the palladium−alumoxane system, i.e., **XVII**.

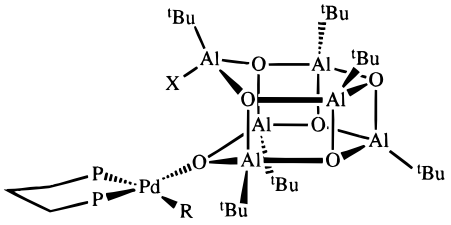

(**XVII**)

While, unlike the case for the zirconocene system, we have no direct evidence for a palladium−alumoxane complex, experimental data and model compounds provide the basis for such a species.

1. The catalytic activity of the palladium−alumoxane system is highly dependent on the polarity (dielectric constant) of the solvent: higher activity is observed in more polar (high dielectric constant) solvents, suggesting that the active catalyst is either highly polar or ionic. However, little or no activity is observed in coordinating solvents. We have shown that the *tert*-butyl alumoxanes are not affected by THF or MeCN,[44] and previous palladium catalysts for polyketone synthesis have been carried out in alcohols and water. Thus, the cessation of catalysis in THF and MeCN cannot be due to decomposition of the alumoxane or inhibition of CO or ethylene complexation but must be due to competitive binding of the solvent in place of the alumoxane.

2. We have not yet been able to obtain structural information on the palladium−alumoxane complexes; however, the reaction of $[(^t\mathrm{Bu})\mathrm{Al}(\mu_3\text{-}\mathrm{O})]_6$ with 2 molar equiv of Cl_3CCO_2H yields the cage-opened alumoxane $[(^t\mathrm{Bu})_6\mathrm{Al}_6(\mu_3\text{-}\mathrm{O})_4(\mu\text{-}\mathrm{OH})_2(\mu\text{-}\mathrm{O}_2\mathrm{CCCl}_3)_2]$, whose structure (Figure 8) has been determined by X-ray crystallography (see below).[45] The structural relationship between the Al_6O_6 core of $[(^t\mathrm{Bu})_6\mathrm{Al}_6(\mu_3\text{-}\mathrm{O})_4(\mu\text{-}\mathrm{OH})_2(\mathrm{O}_2\mathrm{CCCl}_3)_2]$ and that previously reported for $[(\mathrm{Et}_2\mathrm{O})\mathrm{Li}]_2[(^t\mathrm{Bu})_6\mathrm{Al}_6(\mu_3\text{-}\mathrm{O})_6$-

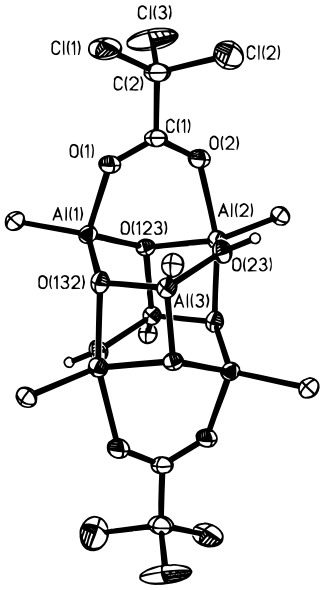

Figure 8. Molecular structure of $[(^t\mathrm{Bu})_6\mathrm{Al}_6(\mu_3\text{-}\mathrm{O})_4(\mu\text{-}\mathrm{OH})_2(\mu\text{-}\mathrm{O}_2\mathrm{CCCl}_3)_2]$. Thermal ellipsoids are shown at the 30% level, and organic hydrogen atoms are omitted for clarity.

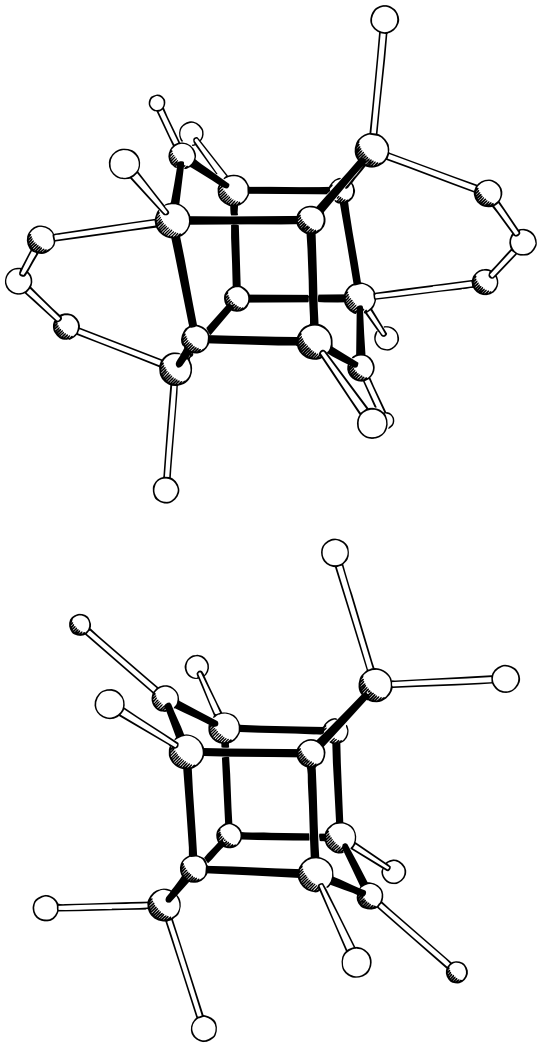

Figure 9. Core structures of $[(^t\mathrm{Bu})_6\mathrm{Al}_6(\mu_3\text{-}\mathrm{O})_4(\mu\text{-}\mathrm{OH})_2(\mu\text{-}\mathrm{O}_2\mathrm{CCCl}_3)_2]$ (top) and $[(\mathrm{Et}_2\mathrm{O})\mathrm{Li}]_2[(^t\mathrm{Bu})_6\mathrm{Al}_6(\mu_3\text{-}\mathrm{O})_6\mathrm{Me}_2]$ (bottom). The solid lines represent the common structural fragments present in each.

(40) (a) Sishta, C.; Hathorn, R. M.; Marks, T. J. *J. Am. Chem. Soc.* **1992**, *114*, 1112. (b) Resconi, L.; Bossi, S.; Abis, L. *Macromolecules* **1990**, *23*, 4489.

(41) (a) Jolly, C. A.; Marynick, D. S. *J. Am. Chem. Soc.* **1989**, *111*, 7968. (b) Lauher, J. W.; Hoffmann, R. *J. Am. Chem. Soc.* **1976**, *98*, 1729.

(42) Dahmen, K. H.; Hedden, D.; Burwell, R. L., Jr.; Marks, T. J. *Langmuir* **1988**, *4*, 1212.

(43) Gassman, P. G.; Callstrom, M. R. *J. Am. Chem. Soc.* **1987**, *109*, 7875.

(44) The high-yield synthesis of $[(^t\mathrm{Bu})\mathrm{Al}(\mu_3\text{-}\mathrm{O})]_n$ is carried out in MeCN solution.

(45) The formation of $[(^t\mathrm{Bu})_6\mathrm{Al}_6(\mu_3\text{-}\mathrm{O})_4(\mu\text{-}\mathrm{OH})_2(\mu\text{-}\mathrm{O}_2\mathrm{CCCl}_3)_2]$ from $[(^t\mathrm{Bu})\mathrm{Al}(\mu_3\text{-}\mathrm{O})]_6$ by the addition of the carboxylic acid to an Al−O bond is similar to the reaction during the formation of carboxylate alumoxanes from the aluminum oxides; see: Landry, C. C.; Pappé, N.; Mason, M. R.; Apblett, A. W.; Tyler, A. N.; MacInnes, A. N.; Barron, A. R. *J. Mater. Chem.* **1995**, *5*, 331.

Me_2] can readily be seen from Figure 9. On the basis of this comparison, and the analogy with [Cp_2ZrMe][(^{t}Bu)$_6$Al$_6$(μ_3-O)$_6$Me] (**XVI**), it is clear that [(^{t}Bu)$_6$Al$_6$(μ_3-O)$_4$(μ-OH)$_2$(μ-O_2CCCl_3)$_2$] represents a suitable model for the interaction of [(^{t}Bu)Al(μ_3-O)]$_6$ with (dppp)Pd(OAc)$_2$.

From the forgoing we propose that the alumoxane forms a complex with the palladium center or a tight ion pair within a solvent cage. This picture is similar to the one we have demonstrated for alumoxanes in zirconocene-catalyzed olefin polymerization. This view of the alumoxane as a coordinating rather than noncoordinating anion is also consistent with the decreased rates of polymerization observed for alumoxane cocatalyzed versus noncoordinating anion cocatalyzed processes.

If the palladium−alumoxane catalyst system is a complex and not discrete ions, then the relative activity of each of the alumoxanes cannot be explained by the relative noncoordinating ability. However, the relative activity of the alumoxanes may be readily understood by a consideration of the alumoxane's latent Lewis acidity and its effects on catalyst activation.

The latent Lewis acidity of a cage alumoxane is its ability to cage-open in the presence of a substrate to provide a Lewis acidic aluminum site. The latent Lewis acidity is dependent on the steric strain imposed upon an Al−O bond by the structure of the cage, Γ_{Al-O}. With a specific substrate, e.g., (dppp)Pd[C(O)R]Cl, there exists an equilibrium between the closed and open forms of the alumoxane, e.g., [(^{t}Bu)Al(μ_3-O)]$_6$ (eq 10). The

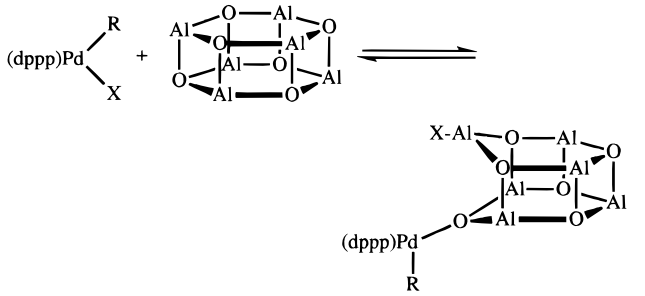

aluminum alkyl groups omitted for clarity (10)

alumoxane/Pd ratio required to activate all the palladium centers to catalysis determines the position of this equilibrium. Thus, in the case of the nonamer and hexamer (Figure 2) the latent Lewis acidity is greater in the latter. The position of this equilibrium is also controlled by the identity of the ligand transferred from the palladium to the aluminum, i.e., the relative bonding energies for the Pd−X and Al−X bonds. This is seen in the observed catalytic activity for (dppp)Pd[C(O)^{t}Bu]Cl being greater than that for (dppp)Pd(OAc)$_2$ (Figure 1). The identity of X may also control the interaction between the alumoxane and palladium fragments; e.g., acetate may possibly act as a bridging ligand between palladium and aluminum.

Molecular Structure of [(^{t}Bu)$_6$Al$_6$(μ_3-O)$_4$(μ-OH)$_2$(μ-O_2CCCl_3)$_2$]. The molecular structure of [(^{t}Bu)$_6$Al$_6$(μ_3-O)$_4$(μ-OH)$_2$(μ-O_2CCCl_3)$_2$] is shown in Figure 8; selected bond lengths and angles are given in Table 3. The Al_6O_6 core structure consists of two fused boat conformation Al_3O_3 rings and can be described as being derived from the opening of two opposing edges of the hexagonal-prismatic core of [(^{t}Bu)Al(μ_3-O)]$_6$. The geometries and bond distances around the Al and O atoms are similar to those we have previously reported for other *tert*-butyl alumoxane compounds. One unusual feature of the structure, however, is the presence of the two five-coordinate aluminum centers, Al(2) and Al(2a). As is common for five-coordinate aluminum, the geometry about Al(2) is that of a distorted trigonal bipyramid: O(2)−Al(2)−O(132a) = 163.7(1)° and $\sum(X_{eq}-Al-X_{eq})$ = 359.6(2)°. The two trichloroacetate ligands each bridge two of the aluminums across opposing six-membered Al_3O_3 faces. The bond lengths and angles within the carboxylate unit are typical of such moieties.[46−48] The ligand bite distance (Al(1)···Al(2) = 3.03 Å) is, however, significantly smaller than those previously observed for aluminum carboxylates (3.26−4.18 Å), with a concurrent decrease in the Al−O−C angles.

Table 3. Selected Bond Lengths (Å) and Angles (deg) for [(^{t}Bu)$_6$Al$_6$(μ_3-O)$_4$(μ-OH)$_2$(μ-O_2CCCl_3)$_2$]

Al(1)−O(123)	1.799(3)	Al(1)−O(132)	1.765(3)
Al(1)−C(11)	1.952(5)	Al(1)−O(1)	1.855(3)
Al(2)−O(123)	1.829(3)	Al(2)−O(23)	1.838(4)
Al(2)−C(21)	1.973(4)	Al(2)−O(2)	2.057(3)
Al(2)−O(13a)	1.999(3)	Al(3)−O(132)	1.778(3)
Al(3)−O(23)	1.815(3)	Al(3)−C(31)	1.945(6)
Al(3)−O(12a)	1.799(3)	O(123)−Al(3a)	1.799(3)
O(132)−Al(2a)	1.999(3)	O(1)−C(1)	1.248(6)
O(2)−C(1)	1.233(6)		
O(123)−Al(1)−O(132)	103.8(1)	O(123)−Al(1)−C(11)	117.7(2)
O(132)−Al(1)−C(11)	124.0(2)	O(123)−Al(1)−O(1)	100.3(1)
O(132)−Al(1)−O(1)	102.8(2)	C(11)−Al(1)−O(1)	104.7(2)
O(123)−Al(2)−O(23)	109.7(1)	O(123)−Al(2)−C(21)	127.6(2)
O(23)−Al(2)−C(21)	122.3(2)	O(123)−Al(2)−O(2)	88.5(1)
O(23)−Al(2)−O(2)	83.6(1)	C(21)−Al(2)−O(2)	91.1(2)
O(123)−Al(2)−O(13a)	80.6(1)	O(23)−Al(2)−O(13a)	88.7(1)
C(21)−Al(2)−O(13a)	105.2(1)	O(2)−Al(2)−O(13a)	163.7(1)
O(132)−Al(3)−O(23)	106.4(2)	O(132)−Al(3)−C(31)	122.3(2)
O(23)−Al(3)−C(31)	111.2(2)	O(132)−Al(3)−O(12a)	87.8(1)
O(23)−Al(3)−O(12a)	101.0(1)	C(31)−Al(3)−O(12a)	124.4(2)
Al(1)−O(123)−Al(2)	118.3(2)	Al(1)−O(123)−Al(3a)	115.6(1)
Al(2)−O(123)−Al(3a)	96.8(1)	Al(1)−O(132)−Al(3)	126.1(2)
Al(1)−O(132)−Al(2a)	121.8(2)	Al(3)−O(132)−Al(2a)	91.6(1)
Al(2)−O(23)−Al(3)	126.1(2)	Al(1)−O(1)−C(1)	128.4(3)
Al(2)−O(2)−C(1)	129.4(3)	O(1)−C(1)−O(2)	126.4(4)
O(1)−C(1)−C(2)	116.7(4)	O(2)−C(1)−C(2)	117.0(4)

Conclusion

The palladium-catalyzed copolymerization of carbon monoxide and ethylene to give polyketone polymers has been accomplished by the use of either (dppp)Pd(OAc)$_2$ or (dppp)Pd[C(O)^{t}Bu]Cl in the presence of *tert*-butylalumoxane cocatalysts.[10] The effects on the catalytic activity of the alumoxane and palladium concentrations suggest that the active catalytic species is a palladium−alumoxane complex. The function of the alumoxane in the catalyst initiation is shown to depend on the choice of palladium catalyst precursor. With (dppp)Pd[C(O)^{t}Bu]Cl the alumoxane abstracts chloride, while with (dppp)Pd(OAc)$_2$ the alumoxane initially alkylates the palladium and subsequently abstracts the remaining acetate anion. The catalytic activity is highly dependent on the structure of the alumoxane employed as the cocatalyst. A comparative study indicates the cocatalytic activity to be [(^{t}Bu)Al(μ_3-O)]$_7$ > [(^{t}Bu)Al(μ_3-O)]$_6$ >

(46) Koide, Y.; Barron, A. R. *Organometallics* **1995**, *14*, 4026.
(47) Sobota, P.; Mustafa, M. O.; Utko, J.; Lis, T. *J. Chem. Soc., Dalton Trans.* **1990**, 1809.
(48) The molecular structure of [(^{t}Bu)$_2$Al(μ-O_2CPh)]$_2$ has been determined by X-ray crystallography: C−O = 1.254(4) and 1.259(5) Å, O−C−O = 122.7(3)°: Barron, A. R. Unpublished results.

$[(^tBu)Al(\mu_3\text{-}O)]_9 \gg [(^tBu)_7Al_5(\mu_3\text{-}O)_3(\mu\text{-}OH)_2]$. This observed cocatalytic activity correlates with the predicted latent Lewis acidity of the alumoxanes, providing further evidence for the intimate association of the alumoxane and the palladium site during catalysis. The steric effects of the catalyst active site, as determined by the alkyl bridge length (n) in $R_2P(CH_2)_nPR_2$ and the alkyl substituents R, were probed for the catalyst precursor compounds $[R_2P(CH_2)_nPR_2]Pd[C(O)^tBu]Cl$. The concept of pocket angle (or interior cone angles) has been developed as an aid to understanding the steric effects of chelating phosphines.

This study has allowed for an understanding of the identity of the active site in the palladium−alumoxane-catalyzed copolymerization of ethylene and carbon monoxide. Our results indicate that consideration of the transition-metal center is not enough. The alumoxane's structure and ability to accept anionic ligands affect activity. The alumoxane thus has a moderating effect on the active site, possibly by complexation to the palladium. A similar effect has been observed for the zirconocene−alumoxane-catalyzed polymerization of ethylene.[12]

Henderson[49] has recently suggested that many metalloenzymatic reactions may be conceptualized from prior knowledge in organometallic chemistry. In contrast, we believe that the cocatalytic function of the alumoxane, and the description of the phosphine "pocket" around the palladium center on which polymerization occurs, requires a view of transition-metal−alumoxane catalyst systems that is closer to that of a metalloenzyme than to traditional transition-metal catalyst systems.

The Lewis acidic abstraction of an anionic ligand from a transition metal (cf. eq 4) is well understood, and we have shown that the ability of any alumoxane to do so is related to its latent Lewis acidity (cf. eq 10). In contrast to previous proposals,[40−43] we propose that instead of acting as a simple noncoordinating anion, the alumoxane is complexed to the "cationic" palladium center during some or all of the steps in the catalytic cycle. Thus, the alumoxane may be thought of as having a stabilizing/cooperating effect on the "cationic" palladium center, in a similar manner to the histidine ligands present in hemoglobin and cytochrome C oxidase.[50,51] The diagrammatic representation of the palladium−alumoxane complex shown in **XVII** may be thought of as a model for a catalyst resting state, with the active state involving dissociation (either partial or complete to form an ion pair) of the alumoxane anion. It is particularly attractive to think of the alumoxane stabilizing the palladium catalyst at the points around the catalytic cycle shown in Scheme 2, where the palladium is shown as being formally three-coordinate. The effective binding of the alumoxane as well as its ability to abstract the ancillary ligand (OAc^- or Cl^-) thus has a major control over the activity of the catalyst system. The size (and possibly shape) of the phosphine's pocket appears to have an effect analogous to that of the amino acid residues in the peptide chain surrounding a metal center in a metalloenzyme. The reverse analogy is commonly used to justify the use of model compounds to study bioinorganic systems.[52] Our future studies will be aimed at further understanding this enzyme-like picture of inorganic transition-metal−alumoxane catalyst systems.

Experimental Section

Copolymerizations were carried out in an autoclave (Berghof, Germany) equipped with a Teflon liner (105 mL). Mass spectra were obtained on a JEOL AX-505 H mass spectrometer operating with an electron beam energy of 70 eV for EI mass spectra. Ammonia was used as the reagent gas for CI experiments unless otherwise mentioned. Infrared spectra (4000−400 cm^{-1}) were obtained using Nicolet 5ZDX-FTIR and Perkin-Elmer 1600 series spectrometers; samples were prepared as CH_2Cl_2 solutions or Nujol mulls. NMR spectra were obtained on Bruker AM-500, Bruker AM-400, and Bruker AM-300 spectrometers using (unless otherwise noted) dichloromethane-d_2.

All synthetic procedures were performed under purified nitrogen using standard Schlenk techniques or in an argon atmosphere VAC glovebox unless otherwise mentioned. Solvents were distilled and degassed prior to use. $[(^tBu)_7Al_5(\mu_3\text{-}O)_3(\mu\text{-}OH)_2]$, $[(^tBu)Al(\mu_3\text{-}O)]_6$, $[(^tBu)Al(\mu_3\text{-}O)]_7$, and $[(^tBu)Al(\mu_3\text{-}O)]_9$ were prepared as previously reported.[14,15] Carbon monoxide, ethylene, and carbon monoxide/ethylene mixture (48.7% CO) gases were obtained from Matheson Gas. (dppp)$Pd(OAc)_2$, dppe, dppb, dmpe, dcpe, $Pd(PPh_3)_4$ (Strem), $^tBuC(O)Cl$, EtC(O)Cl, PhC(O)Cl, and ^tBuMgCl (Aldrich) were used as received. Bis(diphenylphosphino)propane (dppp) was recrystallized from CH_2Cl_2.

$(Ph_3P)_2Pd[C(O)^tBu]Cl$. To a solution of $Pd(PPh_3)_4$ (1.55 g, 1.34 mmol) in toluene (80 mL) was added $^tBuC(O)Cl$ (0.16 mL, 1.40 mmol). The resulting solution was stirred at ambient temperature for 1 h under a dimmed light. Adding Et_2O (80 mL) and cooling to −20 °C yielded a light yellow precipitate, which was filtered and dried under vacuum. Yield: 0.66 g, 66%. ^1H NMR: δ 7.75 (12H, s, *o*-C*H*), 7.39−7.44 (18H, m, *m*-,*p*-C*H*), 0.57 [9H, s, $C(CH_3)_3$].

(dppp)Pd[C(O)^{t}Bu]Cl. $(Ph_3P)_2Pd[C(O)^tBu]Cl$ (0.66 g, 0.88 mmol) was suspended in toluene (50 mL), and dppp (0.36 g, 0.88 mmol) was added. The solution was stirred overnight. Addition of Et_2O (50 mL) gave a pale yellow precipitate, which was recrystallized from CH_2Cl_2. Yield: 0.31 g, 55%. ^1H NMR: δ 7.9−7.5 (8H, br, *o*-C*H*), 7.38 (8H, br, *m*-C*H*), 7.29 (4H, br, *p*-C*H*), 2.58 [2H, q, J(H−H) = 5.0 Hz, $P-CH_2CH_2$], 2.08 and 2.39 (4H, m, P-CH_2), 0.83 [9H, s, $C(CH_3)_3$].

(dppe)Pd[C(O)^{t}Bu]Cl. This compound was prepared using a procedure analogous to that described for (dppp)Pd[C(O)^{t}Bu]Cl. Yield: 40%. ^1H NMR: δ 7.84 (12H, m, *o*-C*H*), 7.74 (6H, m, *p*-C*H*), 7.53 (12H, m, *m*-C*H*), 2.50 (2H, br, $P-CH_2$), 0.88 [9H, s, $C(CH_3)_3$].

(dppb)Pd[C(O)^{t}Bu]Cl. This compound was prepared using a procedure analogous to that described for (dppp)Pd[C(O)^{t}Bu]Cl. Yield: 31%. ^1H NMR: δ 7.67 (12H, m, *o*-C*H*), 7.34 (6H, m, *p*-C*H*), 7.28 (12H, m, *m*-C*H*), 2.4−1.8 (8H, m, CH_2), 0.80 [9H, s, $C(CH_3)_3$].

(dmpe)Pd[C(O)^{t}Bu]Cl. $(Ph_3P)_2Pd[C(O)^tBu]Cl$ (**1**; 0.08 g, 0.11 mmol) was suspended in toluene (70 mL), and dmpe (17.8 μL, 0.11 mmol) was added. The solution was stirred for 3 h, and then Et_2O (50 mL) was added to yield a pale yellow precipitate. The precipitate was collected by filtration and

(49) Henderson, R. A. *J. Chem. Soc., Dalton Trans.* **1995**, 177.
(50) Dickerson, R. E.; Geis, I. *Hemoglobin*; Benjamin/Cummings: Menlo Park, CA, 1983.
(51) Meyer, T. E.; Kamen, M. D. *Adv. Protein Chem.* **1982**, *35*, 105.
(52) See for example: (a) Tang, S. C.; Koch, S.; Papaefthymiou, G. C.; Foner, S.; Frankel, R. B.; Ibers, J. A.; Holm, R. H. *J. Am. Chem. Soc.* **1976**, *98*, 2414. (b) Lane, R. W.; Ibers, J. A.; Frankel, R. B.; Papaefthymiou, G. C.; Holm, R. H. *J. Am. Chem. Soc.* **1977**, *99*, 84. (c) Collman, J. P. *Acc. Chem. Res.* **1977**, *10*, 265. (d) Groves, J. T. *Adv. Inorg. Biochem.* **1979**, *1*, 119. (e) Armstrong, W. H.; Spool, A.; Papaefthymiou, G. C.; Frankel, R. B.; Lippard, S. J. *J. Am. Chem. Soc.* **1984**, *106*, 3653. (f) Spool, A.; Williams, I. D.; Lippard, S. J. *Inorg. Chem.* **1985**, *24*, 2156. (g) Caradonna, J. P.; Reddy, P. R.; Holm, R. H. *J. Am. Chem. Soc.* **1988**, *110*, 2139. (h) Craig, J. A.; Holm, R. H. *J. Am. Chem. Soc.* **1989**, *111*, 2111.

recrystallized from CH_2Cl_2/hexane. Yield: 73%. ^{1}H NMR: δ 1.91 (4H, m, PCH_2), 1.62 (12H, s, PCH_3), 1.15 [9H, s, C(CH_3)$_3$].

(dcpe)Pd[C(O)^{t}Bu]Cl. This compound was prepared using a procedure analogous to that described for (dmpe)Pd[C(O)^{t}Bu]-Cl. Yield: 55%. ^{1}H NMR: δ 2.00 (4H, m, PCH_2), 1.82 (4H, m, β-CH_2), 1.72 (2H, m, δ-CH_2), 1.55 (1H, m, α-CH_2), 1.32 (4H, m, γ-CH_2), 1.23 [9H, s, C(CH_3)$_3$].

$(Ph_3P)_2$Pd[C(O)Ph]Cl. This compound was prepared using a procedure analogous to that described for $(Ph_3P)_2$Pd-[C(O)^{t}Bu]Cl. Yield: 90%. ^{1}H NMR: δ 7.66 (12H, s, *o*-C*H*), 7.55 [2H, m, *o*-C*H*, C(O)Ph], 7.38 (6H, s, *p*-C*H*), 7.29 (12H, m, *m*-C*H*), 7.18 [1H, m, *p*-C*H*, C(O)Ph], 7.00 [2H, m, *p*-C*H*, C(O)-Ph].

(dppp)Pd[C(O)Ph]Cl. This compound was prepared using a procedure analogous to that described for (dppp)Pd[C(O)^{t}Bu]-Cl. Yield: 70%. ^{1}H NMR: δ 7.9−7.5 [10H, br, *o*-C*H*, dppp and C(O)Ph], 7.38 (8H, br, *m*-C*H*), 7.29 (4H, br, *p*-C*H*), 7.10 [1H, m, *p*-C*H*, C(O)Ph], 7.00 [2H, m, *p*-C*H*, C(O)Ph], 2.58 (2H, m, P−CH_2CH_2), 2.0 and 1.8 (4H, m, P-CH_2).

$(Ph_3P)_2$Pd[C(O)Et]Cl. This compound was prepared using a procedure analogous to that described for $(Ph_3P)_2$Pd[C(O)^{t}Bu]-Cl. Yield: 95%. ^{1}H NMR: δ 7.75 [12H, dd, J(P−H) = 12.0 Hz, J(H−H) = 8.0 Hz, *o*-C*H*], 7.46 [6H, t, J(H−H) = 8 Hz, *p*-C*H*], 7.42 (12H, dd, J(H−H) = 8.0 Hz, *m*-C*H*), 1.95 [2H, q, J(H−H) = 7.0 Hz, C(O)CH_2CH$_3$], −0.51 [3H, t, J(H−H) = 7.0 Hz, C(O)CH$_2$CH_3].

(dppp)Pd[C(O)Et]Cl. This compound was prepared using a procedure analogous to that described for (dppp)Pd[C(O)^{t}Bu]-Cl. Yield: 90%. ^{1}H NMR: δ 7.77 (8H, m, *o*-C*H*), 7.47 (12H, m, *m*-,*p*-C*H*), 2.41 [2H, m, P−CH_2CH_2], 1.96 [2H, q, J(H−H) = 8.0 Hz, C(O)CH_2CH$_3$], 1.53 (4H, m, P−CH_2), −0.05 [3H, t, J(H−H) = 8.0 Hz, C(O)CH$_2$CH_3].

Attempted Synthesis of (dppp)Pd(^{t}Bu)(OAc). To a solution of (dppp)Pd(OAc)$_2$ (0.30 g, 0.47 mg) in CH_2Cl_2 (50 mL) was added ^{t}BuMgCl (0.29 mL as 2.0 M Et$_2$O, 0.47 mmol). The resultant berry red solution was added dropwise to hexane (30 mL). A white precipitate was removed by filtration, and then the volume of the filtrate was reduced approximately by half in vacuo. The filtrate was kept at −20 °C to provide ruby red crystals of (dppp)Pd(^{t}Bu)Cl. Yield: <5%. ^{1}H NMR: δ 7.79 (12H, m, *o*-C*H*), 7.53 (6H, m, *p*-C*H*), 7.45 (12H, m, *m*-C*H*), 2.00 (2H, br, P−CH_2CH_2), 2.43 (4H, m, P−CH_2), 0.08 [9H, s, C(CH_3)$_3$].

[(^{t}Bu)$_6$Al$_6$(μ_3-O)$_4$(μ-OH)$_2$(μ-O$_2$CCCl$_3$)$_2$]. [(^{t}Bu)Al(μ_3-O)]$_6$ (300 mg, 0.50 mmol) was dissolved in hexane (5 mL) and the resulting solution added to a solution of HO_2CCCl_3 (82 mg, 0.50 mmol) in hexane (5 mL). After the mixture was stirred for 30 min, a colorless precipitate was formed. Further solid was precipitated by cooling (−24 °C) for 2 h. All of the solid was collected by filtration and then recrystallized from hexane. Yield: *ca.* 40%. IR (cm^{-1}): 2922 (m), 2869 (w), 2869 (m), 2348 (m), 1467 (s), 1285 (m), 1256 (w), 1200 (w), 1121 (m), 1074 (m), 990 (m), 703 (w), 617 (w). ^{1}H NMR (C_6D_6): δ 2.49 (2H, s, O*H*), 1.19 [36H, s, C(CH_3)$_3$], 1.02 [18H, s, C(CH_3)$_3$].

Copolymerization of Carbon Monoxide with Ethylene. In a typical reaction run, alumoxane (0.025 mmol) was placed in the autoclave under an N_2 atmosphere. The autoclave was then purged with dry carbon monoxide gas for 5 min. A stock solution (0.33 mM in dichloromethane) of (dppp)Pd(OAc)$_2$ (15 mL) was transferred into the autoclave under carbon monoxide atmosphere using an appropriate syringe. The autoclave was then pressurized with the reactant gases at room temperature. When carbon monoxide and ethylene were applied separately, carbon monoxide was applied first. The autoclave was placed in a heating unit, and the reaction was carried out at 60 °C with vigorous stirring. At the end of a set period of time, heating was discontinued and the autoclave was cooled to ambient temperature for 10 min before it was disassembled. Following filtration, the product was allowed to dry in air to provide a white powder. Where necessary, the product was washed with hexane (10 mL) and subsequently with CH_2Cl_2 (10 mL).

Table 4. Summary of X-ray Diffraction Data

compd	(dppp)Pd[C(O)^{t}Bu]Cl·CH_2Cl_2	(dppe)Pd[C(O)^{t}Bu]Cl·CH_2Cl_2	(dmpe)Pd[C(O)^{t}Bu]Cl	(dcpe)Pd[C(O)^{t}Bu]Cl·CH_2Cl_2	[(^{t}Bu)$_6$Al$_6$(μ_3-O)$_4$(μ-OH)$_2$(μ-O$_2$CCCl$_3$)$_2$]
emp form	$C_{33}H_{37}Cl_3OP_2Pd$	$C_{32}H_{35}Cl_3OP_2Pd$	$C_{11}H_{25}ClOP_2Pd$	$C_{32}H_{59}Cl_3OP_2Pd$	$C_{28}H_{56}Al_6Cl_6O_{10}$
cryst size, mm	0.21 × 0.23 × 0.54	0.21 × 0.27 × 0.33	0.21 × 0.48 × 0.52	0.32 × 0.34 × 0.38	0.32 × 0.35 × 0.48
cryst syst	monoclinic	monoclinic	monoclinic	monoclinic	triclinic
space group	$P2_1/c$	$P2_1/n$	$P2_1/n$	$P2_1/c$	$P\bar{1}$
a, Å	11.8550(8)	9.5435(6)	10.6837(8)	10.7900(8)	10.202(4)
b, Å	17.200(1)	25.636(2)	11.7098(7)	15.102(1)	10.774(3)
c, Å	16.767(1)	13.777(1)	14.577(1)	22.407(2)	11.517(3)
α, deg					76.78(1)
β, deg	100.318(4)	106.744(6)	109.632(6)	95.237(6)	73.65(1)
γ, deg					86.86(1)
V, Å^3	3363.6(4)	3227.7(4)	1717.6(2)	3636.0(4)	711 82.5(7)
Z	4	4	4	4	1
D(calcd), g/cm^3	1.430	1.462	1.458	1.342	1.299
μ, mm^{-1}	0.902	0.939	1.391	0.835	0.518
radiation	Mo Kα (λ = 0.710 73 Å), graphite monochromator				
temp, K	298	298	298	298	298
2θ range, deg	2.0−44.0	2.0−44.0	2.0−44.0	2.0−44.0	2.0−40.0
no. of collected rflns	4518	4337	2350	4931	2436
no. of indep rflns	4287	4064	2222	4657	2178
no. of obsd rflns	3208 ($\|F_o\| > 6\sigma\|F_o\|$)	2777 ($\|F_o\| > 6\sigma\|F_o\|$)	1593 ($\|F_o\| > 6\sigma\|F_o\|$)	3399 ($\|F_o\| > 6\sigma\|F_o\|$)	1936 ($\|F_o\| > 4\sigma\|F_o\|$)
weighting scheme	$w^{-1} = \sigma^2\|F_o\| + 0.04(\|F_o\|)^2$	$w^{-1} = \sigma^2\|F_o\| + 0.04(\|F_o\|)^2$	$w^{-1} = \sigma^2\|F_o\| + 0.04(\|F_o\|)^2$	$w^{-1} = \sigma^2\|F_o\| + 0.04(\|F_o\|)^2$	$w^{-1} = \sigma^2\|F_o\|$
R	0.0357	0.0457	0.0317	0.0290	0.0461
R_w	0.0378	0.0518	0.0351	0.0298	0.0460
largest diff peak, e Å^{-3}	1.05	0.90	0.39	0.45	0.29

End-Group Analysis for Polyketones Prepared Using (dppp)Pd[C(O)R]Cl. A copolymerization reaction was carried out with (dppp)Pd[C(O)R]Cl and $[(^t\text{Bu})\text{Al}(\mu_3\text{-O})]_6$, under typical reaction conditions (see above), for *ca.* 15 min. The product was filtered and dissolved in $\text{HOC(H)(CF}_3)_2$/benzene-d_6. Any impurities and insoluble materials were removed by filtration before being submitted to mass spectral analysis. Individual volatile oligomers were characterized by GC−MS.

R = ^{t}Bu, Et[C(O)C_2H_4]$_2$C(O)^{t}Bu. MS (EI, %): *m*/*z* 226 (M^+, 100). ^{13}C NMR: δ 35.6 [C(O)*C*H$_2$*C*H$_2$C(O)], 44.3 [C(*C*H$_3$)$_3$], 25.5 [*C*(CH$_3$)$_3$], 33.3 [C(O)*C*H$_2$CH$_3$], 6.7 [C(O)CH$_2$*C*H$_3$].

R = Ph, Et[C(O)C_2H_4]$_n$C(O)Ph. ^{13}C NMR: δ 133.9 (α-*C*, Ph), 131.8 (*p*-*C*H, Ph), 128.9 (br, *o*-,*m*-*C*H, Ph), 35.6 [C(O)-*C*H$_2$*C*H$_2$C(O)], 29.6 [C(O)*C*H$_2$CH$_3$], 6.7 [C(O)CH$_2$*C*H$_3$].

End-Group Analysis for Polyketones Prepared Using (dppp)Pd(OAc)$_2$. This was carried out in a manner analogous to that described above, except (dppp)Pd(OAc)$_2$ was used as the palladium catalyst. The presence of terminal ethyl and vinyl groups was confirmed by ^{13}C NMR: δ 134.0 [−C(O)-*C*H=CH$_2$], 129.1 [−C(O)CH=*C*H$_2$], 29.3 [C(O)*C*H$_2$CH$_3$], 1.2 [C(O)CH$_2$*C*H$_3$]. Individual volatile oligomers were characterized by GC−MS.

CH$_3$CH$_2$[C(O)C_2H_4]$_4$C(O)CH$_2$CH$_3$. MS (EI, %): *m*/*z* 310 (M^+, 10), 281 (M^+ − Et, 20), 253 [M^+ − C(O)Et, 13], 225 [{C(O)C_2H_4}$_3$C(O)Et, 80], 197 [{C_2H_4C(O)}$_3$Et, 65], 141 [{C_2H_4C(O)}$_2$Et, 55], 113 [C(O)C_2H_4C(O)Et, 80], 85 [C_2H_4C-(O)Et, 25].

CH$_3$CH$_2$[C(O)C_2H_4]$_3$C(O)CH=CH$_2$. MS (EI, %): *m*/*z* 251 (M^+ − H, 60), 223 (M^+ − Et, 75), 195 [M^+ − C(O)Et, 40], 169 [{C(O)C_2H_4}$_2$C(O)Et, 30], 141 [{C_2H_4C(O)}$_2$Et, 63], 113 [C(O)-C_2H_4C(O)Et, 100], 85 [C_2H_4C(O)Et, 35].

CH$_3$CH$_2$[C(O)C_2H_4]$_4$C(O)CH=CH$_2$. MS (EI, %): *m*/*z* 308 (M^+, 10), 279 (M^+ − Et, 15), 251 [M^+ − C(O)Et, 31], 223 [{C-(O)C_2H_4}$_3$C(O)CH=CH$_2$, 62], 141 [{C_2H_4C(O)}$_2$Et, 66], 113 [C(O)C_2H_4C(O)Et, 100], 85 [C_2H_4C(O)Et, 29].

Crystallographic Studies. Crystals of (dppp)Pd[C(O)^{t}Bu]-Cl, (dppe)Pd[C(O)^{t}Bu]Cl, (dmpe)Pd[C(O)^{t}Bu]Cl, and (dcpe)Pd-[C(O)^{t}Bu]Cl were sealed in glass capillaries under argon and mounted on the goniometer of the University of North Texas, Department of Chemistry's Enraf-Nonius CAD-4 automated diffractometer. Data collection and cell determinations were performed in a manner previously described,[14] using either the ω or the $\theta-2\theta$ scan technique. Pertinent details are given in Table 4. The structures were solved by Patterson and Fourier methods and the models refined using full-matrix least-squares techniques. A molecule of CH_2Cl_2 was found in the crystal lattice of each structure; however, in the case of (dppp)-Pd[C(O)^{t}Bu]Cl the solvent was disorded, such that the two chlorine atoms were spread over three sites in a 0.85:0.85:0.3 ratio. All non-hydrogen atoms were refined anisotropically, except the low-occupancy chlorine atoms in the dppp compound. Hydrogen atoms were included with fixed thermal parameters and constrained to "ride" upon the appropriate atoms (d(C−H) = 0.95 Å, U(H) = 1.3B_{eq}(C)). All computations were performed using MolEN.[53] A summary of cell parameters, data collection, and structure solution is given in Table 4. Scattering factors were taken from ref 54.

A crystal of $[(^t\text{Bu})_6\text{Al}_6(\mu_3\text{-O})_4(\mu\text{-OH})_2(\mu\text{-O}_2\text{CCCl}_3)_2]$ was mounted in a glass capillary attached to the goniometer head of a Nicolet R3m/V four-circle diffractometer. Data collection and unit cell and space group determination were all carried out in a manner previously described in detail.[55] The structures were solved using the direct methods program XS,[56] which readily revealed the positions of the Al, O, and some of the C atoms. Subsequent difference Fourier maps revealed the position of all of the non-hydrogen atoms. Subsequently, full refinement was successful. All the hydrogen atoms were placed in calculated positions (U_{iso} = 0.08; d(C−H) = 0.96 Å) for refinement. Neutral-atom scattering factors were taken from the usual source.[54] Refinement of positional and anisotropic thermal parameters led to convergence (see Table 4).

Acknowledgment. Financial support of this work was provided by the Office of Naval Research (A.R.B.) and the Robert E. Welch Foundation (S.G.B.). We gratefully acknowledge one of the reviewers for insight into the effect of large pocket angles on catalytic activity.

Supporting Information Available: Full tables of bond lengths and angles and positional and thermal parameters for (dppp)Pd[C(O)^{t}Bu]Cl, (dppe)Pd[C(O)^{t}Bu]Cl, (dmpe)Pd[C(O)^{t}Bu]-Cl, (dcpe)Pd[C(O)^{t}Bu]Cl, and $[(^t\text{Bu})_6\text{Al}_6(\mu_3\text{-O})_4(\mu\text{-OH})_2(\mu\text{-O}_2\text{CCCl}_3)_2]$ (31 pages). Ordering information is given on any current masthead page.

OM9508492

(53) MolEN, An Interactive Structure Solution Program; Enraf-Nonius: Delft, The Netherlands, 1990.
(54) *International Tables for X-Ray Crystallography*; Kynoch Press: Birmingham, U.K., 1974; Vol. 4.
(55) Healy, M. D.; Wierda, D. A.; Barron, A. R. *Organometallics* **1988**, *7*, 2543.
(56) Nicolet Instruments Corp., Madison, WI, 1988.